Lehrstuhl für Raumfahrttechnik
Prof. Prof. h.c. Dr. Dr. h.c.
Ulrich Walter

TECHNISCHE
UNIVERSITÄT
MÜNCHEN

Term Thesis

Payload and Instrumentation Design for an Orbit Knowledge Improvement via Flyby Missions at Asteroids

RT-SA 2015/23
ESA-SSA-NEO-RP-0158

Author:
Stephan Schuster

Supervisor: Dr.-Ing Detlef Koschny
Dipl.-Ing Matthias Tebbe
Lehrstuhl für Raumfahrttechnik / Institute of Astronautics
Technische Universität München

Cover: Artist's impression of Rosetta approaching the comet 67P/Churyumov-Gerasimenko [51]

Erklärung

Ich erkläre, dass ich alle Einrichtungen, Anlagen, Geräte und Programme, die mir im Rahmen meiner Semester- oder Diplomarbeit von der TU München bzw. vom Lehrstuhl für Raumfahrttechnik zur Verfügung gestellt werden, entsprechend dem vorgesehenen Zweck, den gültigen Richtlinien, Benutzerordnungen oder Gebrauchsanleitungen und soweit nötig erst nach erfolgter Einweisung und mit aller Sorgfalt benutze. Insbesondere werde ich Programme ohne besondere Anweisung durch den Betreuer weder kopieren noch für andere als für meine Tätigkeit am Lehrstuhl vorgesehene Zwecke verwenden.

Mir als vertraulich genannte Informationen, Unterlagen und Erkenntnisse werde ich weder während noch nach meiner Tätigkeit am Lehrstuhl an Dritte weitergeben.

Ich erkläre mich außerdem damit einverstanden, dass meine Diplom- oder Semesterarbeit vom Lehrstuhl auf Anfrage fachlich interessierten Personen, auch über eine Bibliothek, zugänglich gemacht wird, und dass darin enthaltene Ergebnisse sowie dabei entstandene Entwicklungen und Programme vom Lehrstuhl für Raumfahrttechnik uneingeschränkt genutzt werden dürfen. (Rechte an evtl. entstehenden Programmen und Erfindungen müssen im Vorfeld geklärt werden.)

Ich erkläre außerdem, dass ich diese Arbeit ohne fremde Hilfe angefertigt und nur die in dem Literaturverzeichnis angeführten Quellen und Hilfsmittel benutzt habe.

Garching, den 30. März 2016

____

Unterschrift

Name: Stephan Schuster
Matrikelnummer: 0362543

Abstract

Incidents like the *Tunguska-Event* (1908) [52] or the *Chelyabinsk Meteor* (2013) [53] illustrate, that the possible impact of an asteroid poses a real threat to Earth and international actions and effective responses are required, in case of an imminent endangerment.

In 2013, the *United Nations Committee on the Peaceful Use of Outer Space* (*UN COPUOS*) reacted to this issue with the establishment of the *Space Mission Planning Advisory Group* (*SMPAG*). The focus of this group lies primarily on the preparation of a global and common response, joint research projects and feasible mission scenarios for the avoidance or mitigation of an asteroid impact [54].

The following thesis shall contribute to this subject and provides estimations for the orbit accuracy, which can be achieved through flyby manoeuvres. Thereby, the uncertainties in orbit computation and propagation are mainly governed by the inaccuracy of the asteroid position measurements. The major source for these data are Earth-based observations, performed by both amateur astronomers and large-scale research centres. However, the measurements obtained from ground-based observations are constrained in precision and some investigations cannot even be conducted from our planet. In contrast to these approaches, a spacecraft which orbits the asteroid or even places a lander on its surface is able to return scientific data with a much higher accuracy and reliability. But the design and implementation of such a rendezvous mission is very complex and, due to limited propulsion resources on the spacecraft, mostly constrained to a single target.

The energy requirements of a flyby mission are generally much lower and potentially allow the exploration of several objects within a single mission. Beyond that, no additional fuel is needed for the deceleration and orbit injection of the spacecraft, which would be necessary in case of a rendezvous mission, whereby a higher payload capacity is available for scientific instruments. Even so, the spacecraft can still operate in close proximity to the asteroid and conduct high-quality measurements. As a result, flybys can be applied to further enhance and augment scientific date from Earth-based observations, without the need for an even more complex and cost-intensive rendezvous mission.

Zusammenfassung

Vorfälle wie das *Tunguska-Ereignis* (1908) [52] oder der *Meteor von Tscheljabinsk* (2013) [53] zeigen, dass ein möglicher Asteroideneinschlag eine reale Gefahr für die Erde darstellt und im Falle einer bevorstehenden Bedrohung ein internationales und effektives Vorgehen notwendig ist.

Das *United Nations Committee on the Peaceful Use of Outer Space (UN COPUOS)* reagierte im Jahr 2013 auf diese Problematik mit der Gründung der *Space Mission Planning Advisory Group (SMPAG)*. Das Hauptaugenmerk dieser Organisation liegt in der Vorbereitung einer globalen und gemeinsamen Strategie, der Kooperation in der Forschung und der Planung von durchführbaren Missionen um Asteroideneinschläge zu verhindern bzw. abzuschwächen [54].

Die vorliegende Arbeit soll zu diesem Thema beitragen und gibt eine Abschätzung darüber, mit welcher Genauigkeit die Trajektorie eines Asteroiden durch Flyby Manöver bestimmt werden kann. Die Ungenauigkeiten in der Orbitberechnung und –vorhersage werden dabei hauptsächlich durch die Unbestimmtheit in den Messungen der Position des Asteroiden bestimmt. Erdgebundene Beobachtungen, durchgeführt von Amateurastronomen sowie großen Forschungseinrichtungen, liefern dabei den größten Anteil an Daten. Diese Messungen sind jedoch in ihrer Präzision eingeschränkt und manche Untersuchungen sind von der Erde aus schlichtweg nicht möglich. Im Gegensatz dazu kann eine Raumsonde, die den Asteroiden umkreist oder sogar eine Landeeinheit darauf absetzt, wissenschaftliche Daten mit einer höheren Genauigkeit und Zuverlässigkeit sammeln. Die Planung und Durchführung einer solchen Rendezvous-Mission gestaltet sich jedoch als sehr komplex und ist aufgrund des limitierten Treibstoffes an Bord des Raumfahrzeuges meist auf ein einzelnes Zielobjekt beschränkt.

Die Energieanforderungen einer Flyby Mission sind im Allgemeinen sehr viel niedriger und erlauben dadurch unter Umständen die Erforschung mehrerer Objekte während einer einzigen Mission. Darüber hinaus wird kein zusätzlicher Treibstoff für das Abbremsen und Einschwenken in den Orbit des Asteroiden benötigt, was Voraussetzung für eine Rendezvous-Mission wäre, wodurch eine höhere Nutzlastkapazität für wissenschaftliche Instrumente zur Verfügung steht.

Die Raumsonde kann dabei trotzdem in unmittelbarer Nähe zum Asteroiden agieren und qualitativ hochwertige Messungen durchführen. Flyby Missionen können somit dazu beitragen, die wissenschaftlichen Daten erdgebundener Untersuchungen zu verbessern und zu erweitern, ohne dass dazu eine äußerst komplexe und kostspielige Rendezvous Mission notwendig ist.

Table of Contents

List of Figures

List of Tables

Symbols

c	[ms^{-1}]	Speed of Light (299,792,458 m/s [25])
δ	[°]	Deflection Angle
Δ	[km]	Impact Parameter
h	[Js]	Planck Constant (6.626 x 10^{-34} Js [25])
G	[$m^3kg^{-1}s^{-2}$]	Gravitational Constant (6.67408 x 10^{-11} $m^3/(kgs^2)$ [25])
r_{SOI}	[km]	Sphere of Influence Radius
m_O	[kg]	Mass of specific Object
m_{Sun}	[kg]	Mass of the Sun (1,988,500 x 10^{24} kg [37])
R	[km]	Distance between Sun and Specific Object
v_∞	[kms^{-1}]	Relative Flyby Velocity

Abbreviations

AU	Astronomical Unit (= 149597870.7 km [25])
BELA	BepiColombo Laser Altimeter
CoF	Centre of Figure
CoG	Centre of Gravity
Delta-DOR	Delta Differential One-Way Ranging
DNS	Deep Space Network
ESA	European Space Agency
ESTRACK	ESA Tracking Stations
Fig.	Figure
JPL	Jet Propulsion Laboratory
KOALA	Knitted Occultation, Adaptive-optics and Lightcurve Analysis
LIDAR	Light Detection and Ranging
MIR	Mid-Infrared
MPC	Minor Planet Center
MPEC	Minor Planet Electronic Circular
NASA	National Aeronautics and Space Administration
NEO	Near-Earth Object
NEOCP	NEO Confirmation Page
NEODyS	NEO Dynamics Site
OSIRIS	Optical, Spectroscopic and Infrared Remote Imaging System
PHO	Potentially Hazardous Object
RSE	Radio Science Experiment
S/C	Spacecraft
SOI	Sphere of Influence
SMPAG	Space Mission Planning Advisory Group
Tab.	Table
UN COPUOS	United Nations Committee on the Peaceful Use of Outer Space
VIRTIS	Visible, Infrared and Thermal Imaging Spectrometer

1 Introduction

This thesis contains a both qualitative and quantitative assessment of a possible payload for an asteroid flyby mission. Different instruments, which can be installed on-board the spacecraft, are evaluated against the background of position and consequently orbit knowledge improvements of the target object.

Chapter 2 gives a brief overview of the theoretical background, in particular the general characterization of asteroids, possible arrangements into different subgroups and their history of origins. Afterwards the process of an asteroid's observation, the collection of its positional data and finally an orbit propagation is shortly illustrated.

The focus of Chapter 3 lies within the comparison between a flyby manoeuvre and the injection of the spacecraft into a bound orbit around the target object. Requirements for both cases are presented, as well as possible benefits or limits regarding the asteroid exploration. Subsequently an overview of previously conducted asteroid flyby missions and their target bodies is given.

For a flyby mission, the accuracy in the asteroid's position determination is governed by both the uncertainty in range between spacecraft and asteroid and the preciseness of the spacecraft tracking from Earth. For the latter one, classical approaches and feasible future enhancements are introduced in Chapter 4.

Section 5 summarizes the main work of the thesis. Thereby, different scientific instruments and experiments, which can contribute to a more constrained position uncertainty, are investigated. The application of such systems in previously carried out space missions is reviewed and necessary modifications for future exploration projects are suggested. For this purpose, the flyby of Rosetta at the asteroid (21) Lutetia in 2010 will serve as an example several times. This is due to the fact that a large number experiments was conducted during the flyby and thus a broad basis of reliable scientific data is available. Beyond that, the instrumentation of future spacecrafts can follow the heritage of the Rosetta and Philae payload, with modifications to the respective mission target.

Finally, Chapter 6 summarizes the results of the thesis and proposes a reasonable instrumentation for an asteroid flyby mission.

2 Theoretical Background

2.1 Asteroid Characterization

About 4.6 billion years ago, our solar system started to form from clouds of gas, which surrounded a protosun [15]. Through the gravitational attraction of dust and gas from the neighbouring interstellar medium, this protosun started to grow and thereby inherited angular momentum from eddies in the interstellar gas [27]. As this accumulation of particles proceeded and the protosun contracted, a disk like nebula formed around it and gained spin. Gravitational forces caused the build-up of particles and the growth of solid objects, called planetesimals, with a size of meters to hundreds of meters. Some collisions of these bodies resulted in the formation of planets, while other collisions lead to the current asteroid and comet population of our solar system.

An asteroid is generally a solid object of the solar system, with dimensions from almost 1000 km down to a few meters and typically consists of rocky material or iron [15]. Objects which also contain volatile, outgassing materials are called comets. They are surrounded by a weak atmosphere, called coma. More massive objects, which have a significant gravitational impact on its environment, are classified as planets and objects smaller than asteroids are declared meteoroids. However, the boundaries of these classifications are not totally strict.

At the beginning, most asteroids moved on nearly circular orbits around the sun. As a result of resonances with the massive planets of the solar system, particularly Jupiter, most of them were deflected onto high elliptical orbits, whereby close encounters with Earth are possible for some asteroids.

This leads to the formation of a subgroup of asteroid, called the *Near-Earth Objects* (*NEOs*). These are asteroids or comets, which orbit the sun with a pericenter distance of less than 1.3 AU. Some NEOs again are classified as *Potentially Hazardous Objects* (*PHOs*). This applies to objects larger than 140 m and an orbital intersection distance with Earth of less than 0.05 AU [15].

Today most asteroids of our solar system are located between Mars and Jupiter in the so called *main belt*. They orbit the sun with a characteristic semi major axis of about 2.2 to 3.3 AU.

NEOs can be generally categorized into four groups, depending on their orbital elements, respectively their apocenter and pericenter distance and eccentricity (see Fig. 2-1). *Amor* NEOs move rather close to Earth but never cross its orbit, while *Apollo* and *Aten* can intersect Earth's trajectory. *Atiras* asteroids are also called *Inner-Earth Objects*, as they always remain inside Earth's orbit and never cross it. The distribution of the detected asteroids into the different groups is very uneven. The majority of the about 14000 known NEOs, as detected until March 2016, is made up of *Apollo* (~54 %) and *Amor* (~38 %) type objects. *Aten* NEOs have a share of only about 7 %, while only 16 *Atira* objects are currently known [28].

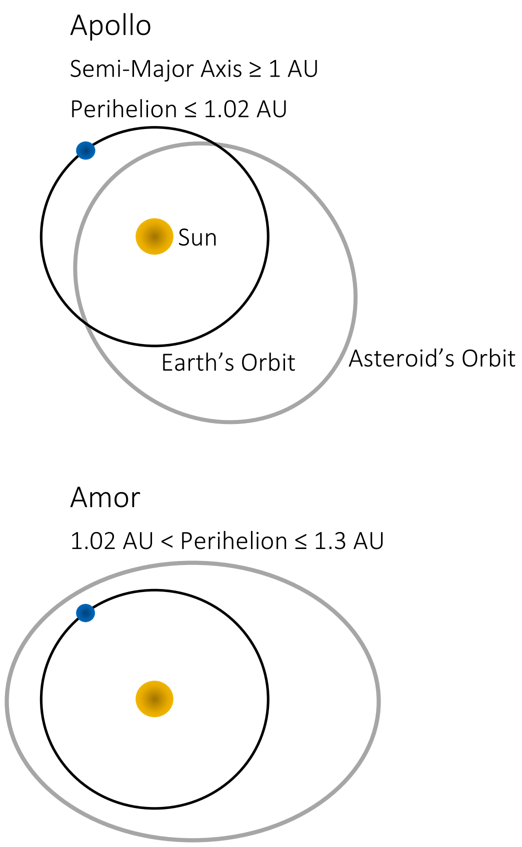

Fig. 2-1: Classification of NEOs depending on their orbital elements [15]

Asteroids can be detected with telescopic observations and appear as illuminated, star like dots. Consequently, their name is derived from the Greek and means "like a star" [15]. Contrary to stars, the observation of asteroids over a longer time span reveals a motion, relative to their background.

Through the measurement of the brightness, first size assumptions for the asteroid can be made. The flux density of the received light, coming from the asteroid is put into relation with a reference object, in most cases the star Vega, and scaled logarithmically afterwards. The resulting parameter is called *magnitude*. Larger values correspond to lower brightness of the object. But the hereby derived size of the asteroid is only a first step estimate. Other effects like the position of the object relative to the Sun and especially the albedo of its surface have a large impact on the observable brightness. The albedo is the percentage of the incoming light, which is reflected and backscattered and strongly depends on the direction towards the light source, the wavelength of the incoming light and the viewing direction. The mean albedo over all these parameters is called *Bond* albedo.

The determination of an asteroid's size is an important step for the estimation of possible impact consequences. A quantitative approach is hereby given by the *Torino-scale,* which uses numbers from 0 (no hazard) to 10 (certain collision) to evaluate the risk and possible danger of an impact.

2.2 Orbit Determination

The detection and subsequent tracking of asteroids is generally done by ground based observations, performed by both amateur astronomers and scientific research centres. The process for the detection of a NEO requires the multiple imaging of the same field in the sky, at different points in time. Typically, 3 to 5 pictures are taken in time intervals of several minutes to half an hour [15]. Applying this method, an asteroid appears as a bright dot, moving relative to the star background. Figure 2-2 presents three images of the asteroid (225254) Flury, detected by the ESA Space Debris Telescope on Tenerife in 2009 [29].

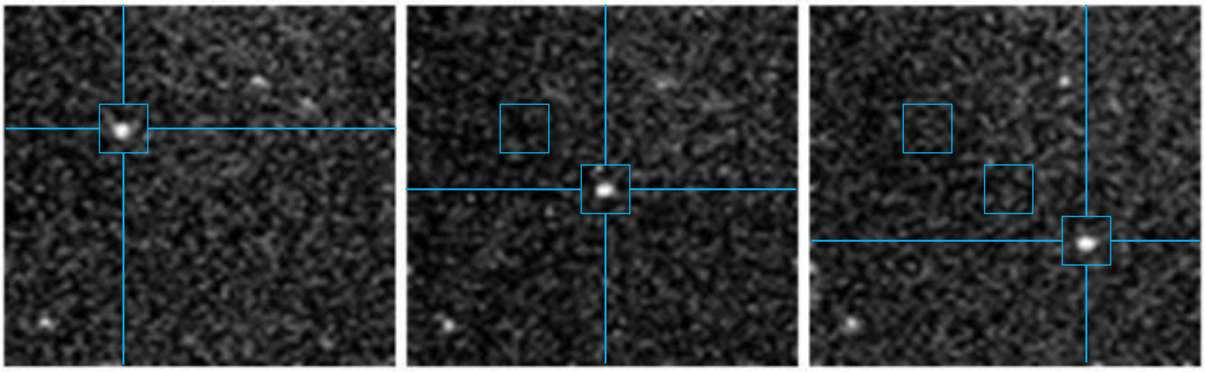

Fig. 2-2: Image series of (225254) Flury taken at time intervals of about 30 minutes [30]

On average, asteroids move with 0.1 – 10 arcseconds per minute in the plane of sky [15]. Their position can be derived from the stars in the background. Thereby the stars, which appear in close proximity to the assumed asteroid, are compared with a star catalogue. Through the relative position of the asteroid to the stars, the position of the asteroid can be determined. This can also be done by specific software programs, which detect moving objects and automatically determine the celestial object of the asteroid.

All measured positon data is then sent to the *Minor Planet Center* (*MPC)* in Massachusetts. This institute collects asteroid position data and observations from all around the world and checks, if they can be matched with an already known object. In case of a new object, a preliminary orbit is computed and an estimation, if the object could be a *NEO* is given. If this probability is larger than zero, the object is officially published on the *NEO Confirmation Page* (*NEOCP).* With these information other observers can perform *follow-up* observations from their position and submit the results again to the *MPC*. Through this process a larger amount of position data can be gathered, which allows a more detailed orbit computation for the object. If these calculations yield that the object is a *NEO*, it is announced in a *Minor Planet Electronic Circular (MPEC)*. The data on this list is now again used for a high accuracy orbit computation which incorporates the propagation of the orbit into the future, in order to detect possible close encounters or even impacts with Earth. These computations are performed separately by the *Sentry System* of the *JPL* and the European *NEO Dynamics Site* operated by the *University of Pisa* [15].

Objects with a non-zero chance of impacting on Earth are put on a *Risk List*, together with estimations on their size and information on when they can be observed again.

Large scale investigation in the light of asteroid detection and observation started only about 20 years ago [15]. As depicted in Fig. 2-3, the number of known and catalogued *NEOs* has significantly increased since then.

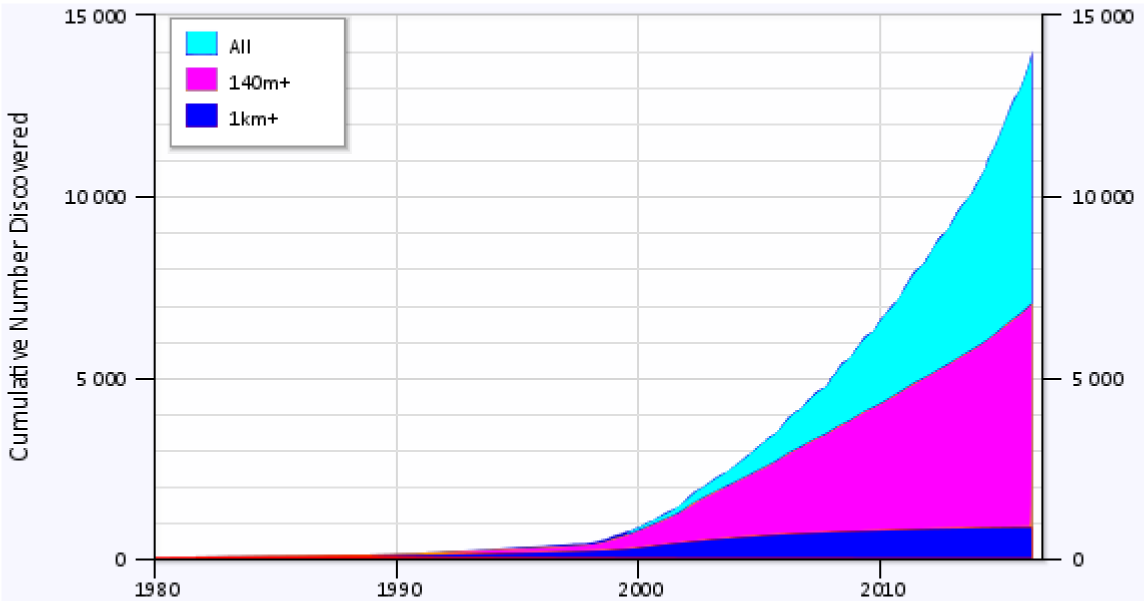

Fig. 2-3: Development of the total number of detected *NEOs* since 1980 [31]

However, due to inaccuracies in the observational data and also non-gravitational forces, which can only insufficiently be determined from ground-based observations, the orbit can often not be computed precisely.

For cases where an accurate and reliable orbit knowledge is absolutely necessary, e.g. when initial calculations indicate a very close Earth flyby or even an impact, position data and ideally further asteroid properties need to be known with a very high accuracy. This may be beyond the possibilities of Earth based observation centres and requires different approaches.

One solution can be the exploration through a spacecraft in proximity to the asteroid. Both a long time observation with a spacecraft in the target object's orbit and the study of the asteroid within the timeframe of a flyby are feasible. Both methods normally allow a more precise position determination and can be used to determine further asteroid properties, which can be only studied insufficiently by Earth based instruments.

3 Asteroid Spacecraft Missions

3.1 Flyby and Bound Orbit Manoeuvres

The most dominant celestial object in our solar system is the Sun. Its large mass and strong gravitational field, impacts the movement and trajectories of all other planets, asteroids and even interplanetary spacecrafts. However, in small distances from an object, its own gravitational field may surpass the attraction of the Sun. This region is called *Sphere of Influence* (*SOI*).

Equation 2-1 gives an estimation for the distance, beyond which the sun's gravitational attraction exceeds the one of the specific celestial object [35].

$$r_{SOI} = R\left(\frac{m_O}{m_{Sun}}\right)^{\frac{2}{5}} \tag{2-1}$$

This parameter is governed by the mass of the object m_O, the mass of the Sun m_{Sun} and the distance R between these bodies. While the masses stay largely constant, the range between the Sun and the object varies along its trajectory. This changes the strength of the Sun's gravitational impact and thereby the *Sphere of Influence.* As presented in Tab. 3-1, a variation of the input parameters can result in significantly different values for r_{SOI}. The input for the calculation was derived from data published by NASA and ESA [37], [38] and [39]. For Earth and Jupiter, their mean distance from the Sun was used for the computation. (21) Lutetia's *Sphere of Influence* was calculated for its position during the Rosetta flyby in 2010.

Tab. 3-1: Overview of the mean *Sphere of Influence* for Earth, Jupiter and (21) Lutetia

Object	Earth	Jupiter	(21) Lutetia
Distance to Sun [AU]	1	5.203	2.715
Object Mass [kg]	5.972×10^{24}	1898.190×10^{24}	1.7000×10^{18}
Sphere of Influence [km]	924644	48209782	6045

Despite its large distance from the Sun, Jupiter shows the highest value for its *Sphere of Influence,* compared to Earth and Jupiter. This is due to its enormous mass, which is several magnitudes higher than one of Earth and especially the one of (21) Lutetia.

Tab. 3-1 shows, that asteroids generally have a rather small *Sphere of Influence*, due to their low mass, and their often large distance from the Sun. This fact must be taken into account for the mission design of a spacecraft, as the gravitational deflection of the probe will be normally very small.

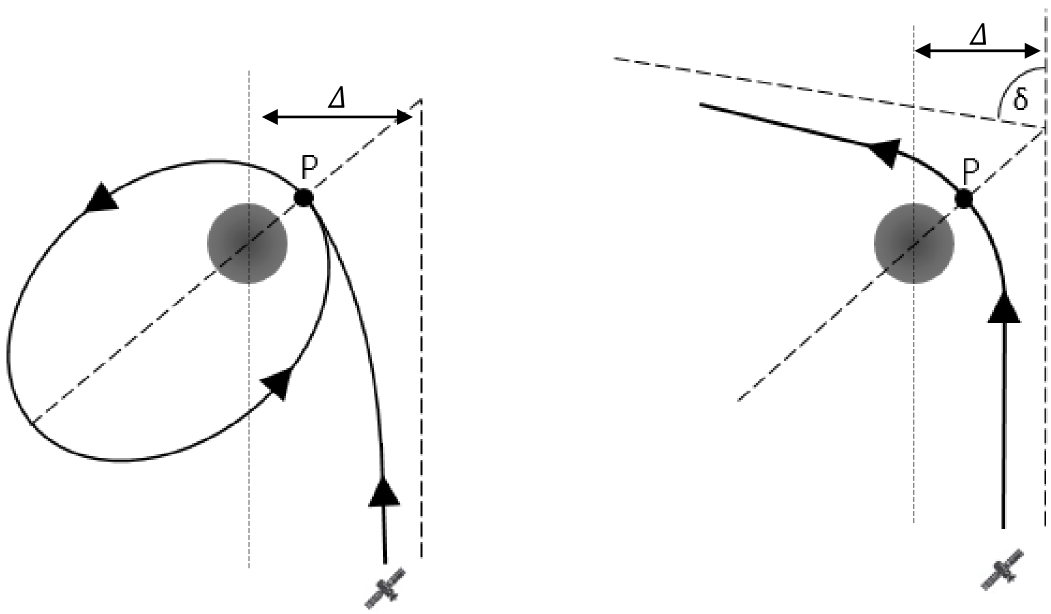

Fig. 3-1: Schematic overview of a spacecraft orbit injection (left) and flyby manoeuvre (right)

Thereby, a spacecraft launched from Earth, arrives at the asteroid's *Sphere of Influence*. As presented in Fig. 3-1, the spacecraft can either fly past the asteroid with some deflection (right image), or drop into an orbit around the object (left image). For the latter, a deceleration is generally required, as the spacecraft arrives at the target with a hyperbolic excess velocity [35]. This is normally done by a *delta-v burn* at the periapsis P. This burn must be very precise and at the accurate height above the target's surface.

If the velocity is not significantly lowered, the spacecraft will simply continue to move along its hyperbolic trajectory and will exit the *Sphere of Influence* afterwards. Depending on the parameters of flyby velocity v_∞, distance Δ mass of the target object M, the spacecraft will be slightly deflected by an angle δ [35].

$$\delta = \pi - 2\tan^{-1}\left(\Delta \frac{v_\infty^2}{GM}\right) \tag{2-2}$$

The most accurate and reliable data can normally be derived from a spacecraft orbiting the asteroid [15]. Thereby the target body can be investigated through long time observations, which also allow the observation from many different points of view and the exploration of the whole surface. More experiments can be conducted through the additional deployment of a lander on the target's surface.

On the contrary, flybys normally allow only a short time of observation, as both the relative velocity between asteroid and spacecraft is in the range of a few km/s and the spacecraft passes the object only once. The adequate flyby distance must be a trade-off between several aspects. On the one hand, passes at low altitudes present the risk of a possible collision with the object, while they often allow more precise and detailed measurements (e.g. camera, mass determination with RSE). On the other hand, it may be challenging for some instruments to track the asteroid because of the high slew rates during close encounters. This can result in uncertainties of the measurements.

Nevertheless, flyby mission at asteroids may be a promising method for the exploration of asteroids. They allow scientific measurements in close proximity to the object, with a normally significantly higher accuracy than obtained from Earth-based measurements, and are less elaborate than orbiting missions. This comes from the high precision, which is needed for the manoeuvring and deceleration of a spacecraft in order to inject it into a bound and stable orbit. Beyond that, for the in-orbit deceleration a huge amount of additional fuel is needed, which again increases the mass and decreases the payload for additional scientific instruments. Moreover, orbiting missions are often bound to one target, as the spacecraft cannot gain the necessary velocity to leave one asteroid's orbit and then fly to another one. However, flyby manoeuvres can often be easily added to missions and perhaps even allow the encounter with several objects.

3.2 History of Asteroid Flyby Missions

During the last 25 years, six different spacecraft performed flybys at various asteroids. An overview of the missions can be seen in Tab. 3-2. The data is derived from [12], [22], [32], [33], [34], [41], [58] and [59]. This table only depicts actual flybys, whereas asteroid landings are not included. Also several missions to comets or other small objects in the solar system, e.g. *Phobos,* are not included, although such missions will have a similar design.

The table provides information on the target of the mission, its mass and overall dimensions. The flyby at (2867) Steins (5535) Annefrank provided no reliable measurement for the mass of the body, due to their small size and the additionally large flyby distance. The size of the visited asteroids varies largely from massive objects, with over 100 km ((21) Lutetia), to very small objects ((4179) Toutatis, (9969) Braille), with only a few kilometres in diameter. But also the latter ones pose a potential risk to Earth and can cause global damage. Thereby their exploration is necessary, too.

Tab. 3-2: Overview of conducted asteroid flyby missions

Chang'E-2 - CNSA			
Flyby Date	Target Object	Target Mass [kg]	Target Diameter [km]
13.12.2012	(4179) Toutatis	0.05×10^{15}	4.6 x 2.4 x 1.9
Rosetta - ESA			
Flyby Date	Target Object	Target Mass [kg]	Target Diameter [km]
10.07.2010	(21) Lutetia	1700×10^{15}	124 x 101 x 80
Flyby Date	Target Object	Target Mass [kg]	Target Diameter [km]
5.09.2008	(2867) Steins	-	6.8 x 5.7 x 4.4
Stardust - NASA			
Flyby Date	Target Object	Target Mass [kg]	Target Diameter [km]
2.11.2002	(5535) Annefrank	-	4.8
Deep Space 1 - NASA			
Flyby Date	Target Object	Target Mass [kg]	Target Diameter [km]
29.07.1999	(9969) Braille	0.0078×10^{15}	2.2 x 1.0
NEAR Shoemaker - NASA			
Flyby Date	Target Object	Target Mass [kg]	Target Diameter [km]
27.06.1997	(253) Mathilde	103.3×10^{15}	66 x 48 x 46
Galileo - NASA			
Flyby Date	Target Object	Target Mass [kg]	Target Diameter [km]
28.08.1993	(243) Ida	100×10^{15}	58 x 23
Flyby Date	Target Object	Target Mass [kg]	Target Diameter [km]
29.10.1991	(951) Gaspra	10×10^{15}	19 x 12 x 11

4 Spacecraft Tracking Accuracy

For the determination of an asteroid's orbit through a space mission, it is important to have reliable and accurate data for the position of the spacecraft itself. Until the 1980s the tracking methods for deep space missions relied almost exclusively on the radiometric techniques of ranging and Doppler measurements [1]. Until today, these methods are the basis of modern spacecraft tracking. However, over time modifications and new (radiometric) tracking methods have enhanced the achievable accuracy and could thereby be implemented for future asteroid missions, too.

4.1 Radiometric Range and Doppler Measurements

The radiometric tracking of a spacecraft is normally performed by the Earth-based, deep space antennas of NASA's Deep Space Network (DSN) [1] or ESA's tracking stations (ESTRACK) [8]. Both systems consist of numerous stations, widely separated around the globe, which can transmit commands and receive data.

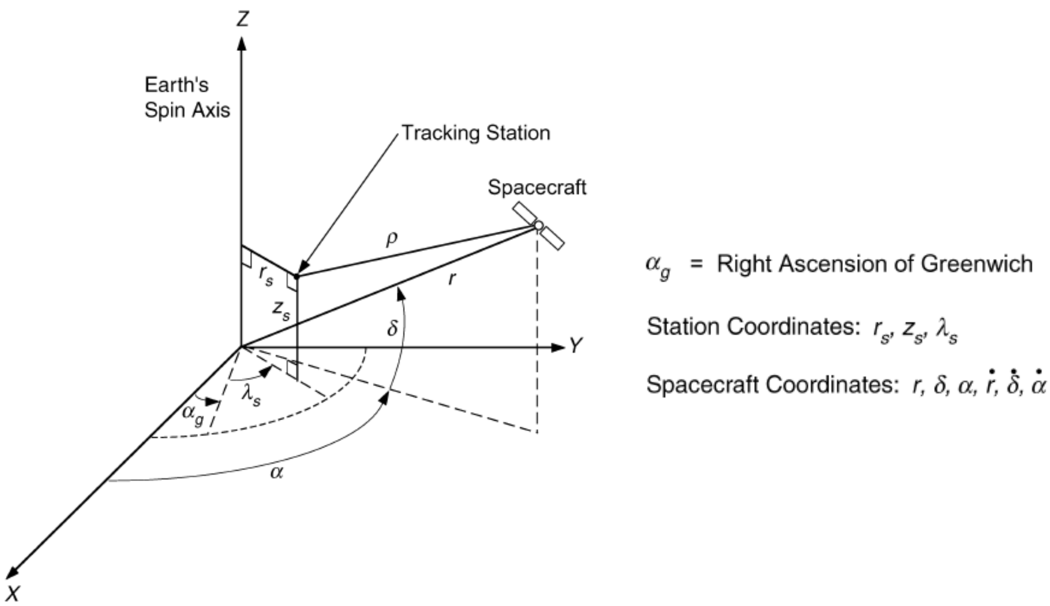

Fig. 4-1: Spacecraft and ground station coordinates in a geocentric system [1]

The position of a spacecraft, respectively its trajectory, relative to the earth, can be described by a state vector in a geocentric system, consisting of six parameters (see Fig. 4-1).

For a complete determination of a spacecraft's current position, its geocentric range r, right ascension α and its declination δ need to be measured. Additionally, the respective velocity components $\dot{r}$, $\dot{\alpha}$ and $\dot{\delta}$ must be known for a precise orbit determination and propagation. As the spacecraft's position and movement is tracked from the Earth's surface, the measured data is relative to the position and velocity of the observing station. With the knowledge of the ground station's coordinates, the spacecraft position can then be transferred into the final geocentric system.

The most precise ranging measurements can be achieved via a two-way tracking mode, where the ground station transmits a signal to the spacecraft, which is then sent back and received by the same tracking station [1]. For some deep space missions, with extremely large distances between Earth and spacecraft, this method may not be applicable. This is due to the fact, that the time-span in which the signal travels to the spacecraft and back, the receiving station is already out of view, due to Earth's rotation. In this case a second ground station is necessary for the reception. This method is called three-way tracking. As future asteroid missions may operate in a large distance from Earth, a three-way tracking probably has to be applied in some cases.

The line of sight distance ρ between the tracking station and the spacecraft for a two-way tracking can be calculated with the following formula:

$$\rho = \frac{1}{2}\tau_g c \tag{4-1}$$

This equation is based on the precise measurement of the two-way signal transit time τ_g and the speed of light c [1]. But as the Earth rotates between the transmission and the reception of the signal by the ground station, the upload path of the signal differs from the downlink path. However, since the rotation rate of the earth, the signal transit time and the location of the tracking station is normally well known, this problem can be solved through rather simple geometric calculations.

Apart from the transit time, the frequency shift between the transmitted and received microwave can be measured, too. Based on theory of the Doppler-effect, the spacecraft receives a signal with a different frequency than it was originally transmitted from the ground station, as long as there is a relative velocity between these two objects.

$$f_R = \left(1 - \frac{\dot{\rho}}{c}\right) f_T \tag{4-2}$$

In this equation f_T is the frequency of the signal communicated by the spacecraft, while f_R is the frequency of the signal as it is received by the tracking station [1]. This calculation is used for the determination of the spacecraft instantaneous slant range rate $\dot{\rho}$, which is the relative line of sight velocity between the tracking station and the spacecraft.

The distance and velocity measurements with the above described techniques are very reliable, and allow the determination of the spacecraft's state with an error of about 1 m in range and less than 0.1 mm/s in range rate [3]. However, these methods deliver only the values along the line of sight, but give no information about the angular position coordinates against the sky background. For a complete position determination, the right ascension and the declination of the spacecraft must be known. However, these two parameters can be only derived indirectly from the range and range rate measurements.

$$\dot{\rho}(t) = \dot{r}(t) + \omega_e r_s \cos(\delta)\sin(\omega_e t + \phi + \lambda_s - \alpha) \qquad (4\text{-}3)$$

The slant range rate $\dot{\rho}$ at any instant of time can be closely approximated by equation 4-3 [1]. Hereby, the values for the longitude of the tracking station λ_s, the distance of the tracking station from Earth's spin axis r_s and the mean rotation rate of Earth ω_e need to be known. The geocentric range rate $\dot{r}$ can be expressed by the identified geocentric state vectors of the tracking station and the slant range rate $\dot{\rho}$. If civil time at Greenwich is used for t, then ϕ, which represents the phase angle that depends on the epoch, corresponds to the instantaneous right ascension of the sun.

Thereby, only the right ascension α and the declination δ are unknown. These parameters can now be derived indirectly from diurnal radiometric observations.

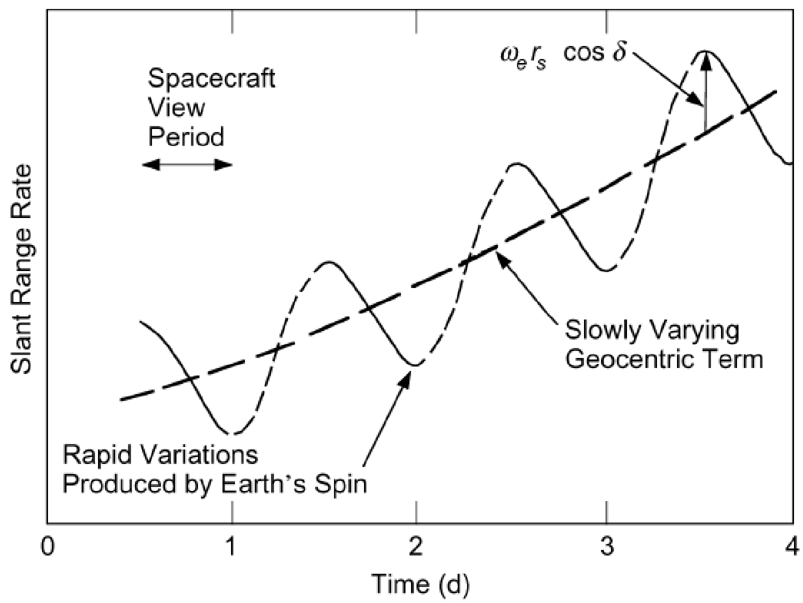

Fig. 4-2: Detected Doppler signature for an observation period of several days [1]

Figure 4-2 gives and impression of the received slant range rate during a longer observation of the spacecraft [1]. In an idealized form, this illustration is a sinusoid, superimposed upon a ramp function. The ramp function represents the geocentric velocity of the spacecraft. The sinusoid function which is detected at the ground, is due to the rotation of the tracking station around Earth's spin axis. As mentioned above, this function can be modelled and approximated with equation 4-3. The amplitude of this sinus function is given by $\omega_e r_s \cos(\delta)$ and can be seen in figure 4-2. Thereby the declination δ can be obtained from the measured data. Finally, the only unknown parameter remaining, the right ascension α of the spacecraft, can be calculated via equation 4-3.

But as the angular position of the spacecraft can only be measured indirectly, the right ascension and declination can only be determined with a rather larger error of about 0.17 mrad [2]. For critical stages of a space mission, e.g. swing-by or landing phases, this angular accuracy may not be sufficient and also for an absolute precise position determination of an asteroid, a higher accuracy in plane-of-sky position is desirable.

4.2 Optical Methods and Delta Differential One-Way Tracking

Thereby, cameras on-board the spacecraft can be used for tracking purposes and position determinations, too. Images are taken from a reference object, for instance an asteroid, and provide a line-of-sight vector to that body. The direction of this vector can then be determined via the stars in the background of the picture. Their position is normally known very accurately and stored in star catalogues. A sequence of multiple images with slightly different viewing angles is then evaluated and a non-linear least square filter is applied, which estimates the spacecraft's position and velocity [55]. Contrary to the radiometric range and range-rate measurements, the optical system determines the angular position directly, which allows angular accuracies in the range of 1.7 µrad [2]. The application of optical navigation techniques is especially recommended for the approach and flyby phase and was also utilized during Rosetta's encounter with (21) Lutetia [56]. Prior to this the asteroid's position was determined via ground-based astrometric observations and thereby independently from the position of the spacecraft, which was tracked with radiometric techniques [2]. Optical navigation can now provide a direct relation between the spacecraft's and the asteroid's position. Consequently, the augmentation of radiometric tracking techniques by optical navigation should be considered, especially in the case of an approaching target.

In order to achieve higher angular accuracies with radiometric techniques other strategies have to be applied. One of the most promising methods is the Delta Differential One-Way Tracking (delta-DOR or DDOR). In this case, the range and the range rate are measured in the same way as described in the previous chapter. However, the angular position can now be determined directly. Thereby methods like delta-DOR augment the classical approach by using two widely separated antennas, which simultaneously track the incoming signal of a spacecraft, as depicted in Fig. 4-3. As the distance of the spacecraft is very large, compared to the distance between the two ground stations, the signals of the spacecraft can be approximated parallel [1]. The line-of-sight range between the ground stations is called the baseline B.

The signals now arrive at the different tracking stations at different instants of time. This difference is called delay time and can be transferred into a distance by multiplying with the speed of light. With equation (4-4) one angular component of the spacecraft position can be calculated using the baseline length B and the time delay $\rho_2 - \rho_1$ [1].

$$\rho_2 - \rho_1 = B \sin \delta \tag{4-4}$$

A combination of data, obtained by different stations with different baselines provides a complete set of the angular position of the spacecraft. The best results can be derived from different tracking stations, if their baselines are very large and preferably perpendicular to each other. The Deep Space Network is capable of such measurements and provides accurate position data since the 1980s [1]. With ESA's two deep space antennas in Cebreros (Spain) and New Norcia (Australia) the simultaneously tracking is also possible. But again, in order to determine a second angular component, at least one additional antenna must be used.

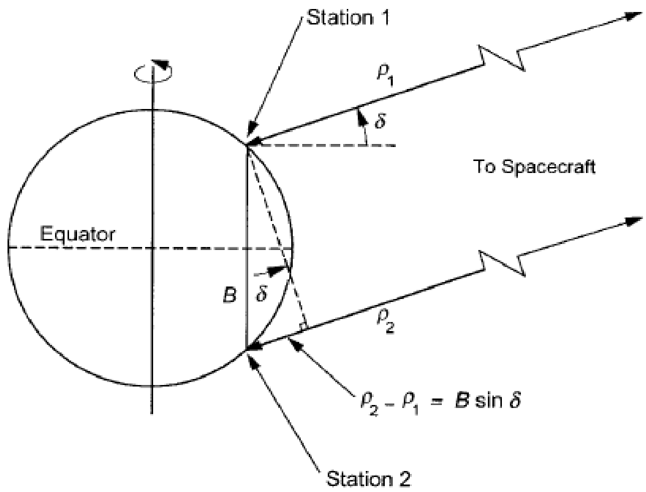

Fig. 4-3: Simultaneous spacecraft tracking using two different ground stations [1]

Idealized the delay depends only on the distance between the spacecraft and the antennas. In reality error sources, e.g. perturbations caused by the troposphere, ionosphere or solar plasma deteriorate the measurements. These errors can be directly quantified with the delta-DOR method. Thereby a quasar in a direction close to the spacecraft is tracked (see Fig. 4-4). Through astronomical measurements, its position is normally known extremely accurate, with an accuracy of up to 1 nrad [2].

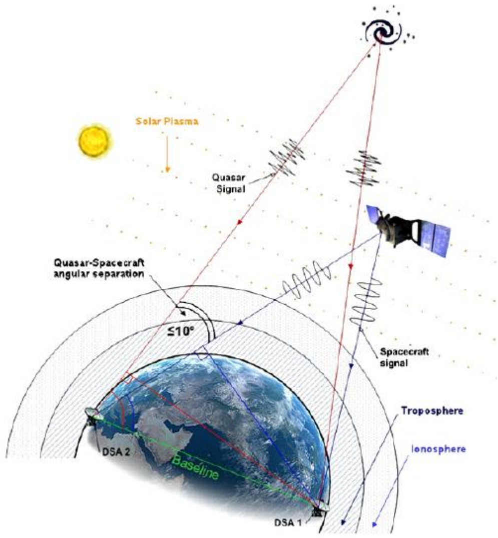

Fig. 4-4: Calibration of measurement errors by the tracking of a quasar [4]

Consequently, the delay time of the quasar is subtracted from the one of the spacecraft in order to compensate for the measurement perturbations of the spacecraft [4].

The delta-DOR tracking method augments range and range rate measurements by providing a direct way of quantifying the angular components of the spacecraft's position. ESA's system was already successfully applied during the Venus Express Mission in 2006 or Rosetta's Mars swing-by in 2007 [3].

As delta-DOR provides a direct measurement of the angular position of a spacecraft it achieves much higher accuracies than other methods. The limiting factor is the exact measurement of the time delay, which can be measured with up to 1 ns uncerainty. This corresponds to a deviation of only about 25 nrad. This means, that for a spacecraft in a distance of about 1 AU the uncertainty is less than 4 km [4]. For the near future even an uncertainty of about 1.4 nrad seems feasible [7], which again would correspond to a position uncertainty of less than 300 m in 1 AU distance (see Tab. 4-1)

The application of delta-DOR is an attractive way for future space missions and also for asteroid flyby manoeuvres. With these enhanced methods the position of a spacecraft can be determined with an error in the range of a few hundred meters, even in very large distances from the ground stations. This would again help for a better estimation of the asteroid's orbit and position.

A crucial part of the communication between spacecraft and ground station is the used frequency bands of the signal. Studies and recent space missions have shown that signals with a higher frequency, X-band (8.4 GHz) and especially Ka-band (32-34 GHz), are less affected by charged particles of the ionosphere and solar plasma and thereby reduce the error of the measurements. Thus, the application of these uplink and downlink frequencies to deep space probes can be recommend and will result in an improvement of the radiometric measurements [1].

Tab. 4-1: Qualitative comparison of achievable angular accuracies [2], [4], [7]

Technique	Range Rate	Optical	Delta-DOR	Delta-DOR
Measurement Method	Indirectly	Directly	Directly	Directly
Operational Capability	Already Applied	Already Applied	Already Applied	Feasible
Angular Accuracy [nrad]	170000	1700	25	1.4
Uncertainty at 1 AU [km]	25431.64	254.32	3.74	0.21
Uncertainty at 2 AU [km]	50863.28	508.63	7.48	0.42
Uncertainty at 3 AU [km]	76294.91	762.95	11.22	0.63

5 Payload and Instrumentation

For the exploration of asteroids, various types of instruments can be integrated into the spacecraft. Tab. 5-1 presents an overview of possible experiments and the respective asteroid property, which can be determined, for different asteroid approaches (e.g. Flyby, Lander). Tab. 5.2 shows, which instrumentation is necessary for the determination of a specific asteroid property. Within this thesis, only experiments which directly contribute to an improvement in position and orbit knowledge are considered.

Tab. 5-1: Possible mission payload and thereby characterized properties [10]

	Earth-based	Flyby		Orbiter		Orbiter + Lander
Mass	Indirect estimate (volume and assumed density), unless binary	Radio science		Detailed Radio Science Experiment		
Centre of gravity	Assumed as the centre of figure	Centre of figure + radio science		Detailed RSE, radar tomography		+ seismometers
Size, Shape, Spin, Multiplicity	Radar, AO imaging, ligthcurves, radiometry	Direct imaging	May not cover the whole body	Direct imaging + altimeter		
Composition	VIS-NIR-MIR spectroscopy	Surface mapping	VIS-NIR-MIR spectroscopy	Surface mapping. X-ray spectroscopy?	VIS-NIR-MIR spectroscopy	+ Mössbauer, Raman, X-ray, gamma-ray spectroscopy
Albedo	Radiometry, polarimetry	Cameras and MIR spectroscopy		Cameras and MIR spectroscopy		
Surface porosity	Polarimetry, radar, MIR spectroscopy	Polarimetry, radar, MIR spectroscopy, hints from surface features		Polarimetry, radar, MIR spectroscopy, hints from surface features		+ Penetrator science
Thermal properties	MIR spectroscopy or photometry	MIR spectroscopy (surface resolved)	May not cover the whole body	MIR spectroscopy (surface resolved)		+ Thermal sensor, penetrator science
Mechanical properties	Assumed from thermal properties and laboratory measurements of surface analogues	Assumed from thermal properties, laboratory measurements of surface analogues, hints from surface features		Assumed from thermal properties, laboratory measurements of surface analogues, hints from surface features		+ Penetrator science
Bulk density	Assumed from surface analogues, unless binary: indirect estimate from mass and volume	From mass and volume		From mass and volume		
Porosity, Internal structure	Assumptions from rotational properties, radar observations, surface analogues	Assumptions from rotational properties, radar observations, surface analogues, hints from surface features		Radar tomography		+ seismometers

Tab. 5-2: Necessary instrumentation for the respective asteroid parameter [9]

	Mass	Orbit	Gravitational Field	Rotation Properties	Size and Shape	Near-surface Properties	Topography and Morphology	Mineralogy	Elemental Composition
Radio Science	■	■	■			■			
Imagers				■	■	■	■		
LiDAR			■		■		■		
Thermal IR Spectrometer		■				■		■	
Visible Near IR Spectrometer						■		■	
X-Ray Spectrometer									■
Radar Tomographer			■			■			
Seismic Experiment			■			■			

5.1 Radio Science Experiments

The determination of an asteroid's mass is principally done via the observation of its gravitational impact on other bodies. Thereby the asteroid causes a perturbation of the orbit of another celestial object. But as an asteroids mass is generally insignificant, compared to planets or the Sun, accurate mass estimations with Earth-based observations can only be performed by the analysis of the gravitational impact on other asteroids. For rather large objects like Ceres, Pallas or Vesta, this method delivers accurate results, with an error in mass of only a few percent. However, it lacks accuracy for smaller objects. Even for quite massive asteroids with dimensions of about 100 – 150 km, the uncertainties can be higher than 100 % [10]. Using Earth-based observations, the most precise results can be obtained for binary systems through the assessment of the gravitational perturbation of an asteroid on its satellite. And yet the reached accuracies of this method, of about 10 – 15 % [10], are not sufficient for a reliable improvement of long-term asteroid ephemerides [13]. Better estimations can be provided through the analysis of a spacecraft visiting the asteroid, which allows the determination of the asteroid's mass with accuracies of up to 1 % [12].

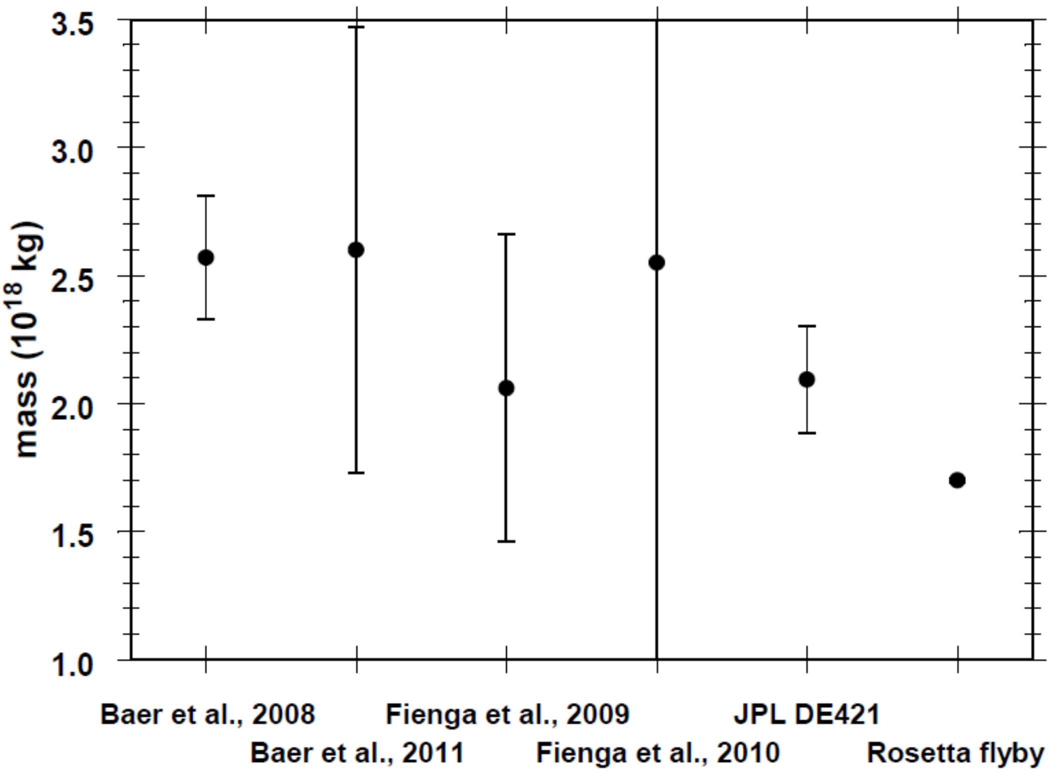

Fig. 5-1: Evolution of mass estimations for (21) Lutetia with the respective uncertainty [10]

Fig. 5-1 presents several mass estimations for the asteroid (21) Lutetia. While previous ground-based analyses (see Fig. 5-1: Baer 2008, Baer 2011, Fienga 2009, Fienga 2010 and JPL DE421) contain a large error, the Rosetta flyby in 2010 provided an accurate determination of the mass of (1.700 ± 0.017) x 10^{18} kg, which corresponds to an uncertainty of only 1 % [12]. The respective error bar of the Rosetta mass determination is not large enough to be visible in Fig. 5-1.

During such a flyby, the gravitational force of the asteroid constantly perturbs the trajectory of the spacecraft and causes a change in its velocity. This again results in a Doppler frequency shift of the transmitted radio signal.

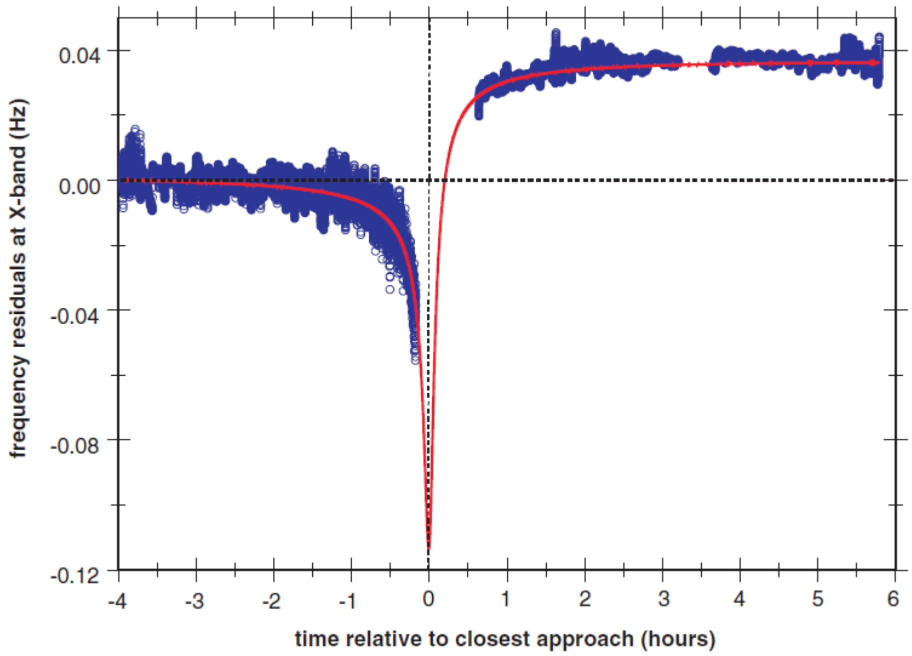

Fig. 5-2: Received frequency residuals from Rosetta during the (21) Lutetia flyby [12]

Fig. 5-2 presents the residuals of the received radio signal during the (21) Lutetia flyby from four hours before, to six hours after the closest encounter. The blue line in the plot shows the received frequency minus the expected frequency of a probe not disturbed by any force. The red line presents the frequency residuals after the least-square fit. Hours before the flyby, the received and expected (undisturbed) signals are identical. As the spacecraft approaches the asteroid the increasing gravitational force causes a growing change in velocity and consequently frequency. After the spacecraft has flown by the asteroid and the gravitational impact is no longer significant, the frequency again stays constant. The difference between the radio signal without perturbation and the received signal long time after the flyby is called *final postencounter Doppler shift* [12]. This frequency change is mainly governed by the flyby distance d, the relative velocity between spacecraft and asteroid v_0, the flyby geometry, expressed by α' and β and of course the mass M of the asteroid [14]. It can be expressed by the following term [12]:

$$\Delta f(t \to \infty) = 4 \frac{f_x}{c} \frac{GM}{d v_0} \sin(\alpha') \cos(\beta) \tag{5-1}$$

The detected Doppler shift is proportional to the mass and also the frequency, thus the installed on-board frequency band. As the gravitational field of an asteroid is rather weak, the spacecraft should be equipped with a dual band link with high frequencies (X- and Ka-bands) in order to achieve high accuracies [9]. The frequency shift is also inversely proportional to the relative flyby velocity and the distance between spacecraft and asteroid at closest encounter. Beyond that, the geometry of the flyby manoeuvre has a large impact on the Doppler shift and thus the achievable accuracy. The Doppler shift, which can be observed from Earth is the one along the line-of-sight between ground station and spacecraft. As the trajectory of the spacecraft is normally not identical to the line-of-sight the correction angels α' and β must be implemented in order to describe the flyby geometry correctly and thereby determine the mass of the asteroid accurately.

Thereby α' is the angle between the trajectory of the spacecraft and the projection of the line-of-sight, between spacecraft and ground station, into the flyby plane. The flyby plane however is determined by the asteroid centre of mass and the relative velocity vector of the manoeuvre. The angle between the flyby plane and the direction angle to the ground station is β. The most precise data can be derived for α' = 90° and β = 0°. This represents a movement along the line-of-sight and allows the detection of the total velocity change. Due to constraints of the mission design and the consequent spacecraft trajectory, this ideal case will be applicable only very rarely. However, if the parameters of the mission allow different flyby paths at the asteroid, a movement close to the line-of-sight is preferable, as the total frequency shift can be detected and the mass can be estimated with a higher accuracy.

For an accurate determination of an asteroid’s mass, other influences on the spacecraft, e.g. attraction by other planetary bodies or other asteroids, and non-gravitational forces acting upon it must be taken into account, too. For a flyby manoeuvre the main cause of the latter is solar radiation pressure. Thereby the emitted photons from the sun are partially absorbed and reflected by the spacecraft. This effect changes the trajectory and the velocity of the spacecraft additionally and causes a further frequency shift [11]. As the gravitational force decreases with larger distance, the solar radiation pressure can even surpass the asteroids gravitational field in such cases. But as this has nothing to do with the asteroid, it can lead to wrong mass estimations and its share of the frequency shift has to be subtracted from the received signal.

Basically two different approaches for the consideration of the solar radiation pressure exist. The first one is the modelling of the perturbation of the spacecraft, depending on the incoming solar radiation pressure, respectively photons. The occurring force depends primarily on the amount of impinging photons on the spacecraft and their energy [11] and thereby changes with distance from the Sun and the pointing angle of the spacecraft towards it. However, within this method the influence of the solar radiation pressure can only be guessed and not directly measured. Thus, false models and not considered effects could result in inaccurate assumptions for the solar pressure and lead to wrong mass estimations. Though no additional on-board instruments are needed for this, it may be a sufficient solution for flybys with an insignificant impact of the incoming photons. This applies for example to large asteroids or close encounters.

If these effects cannot be foreseen or results with a very high accuracy are demanded, the Radio Science Experiment can be augmented by an accelerometer [9]. This means an additional payload and the centre of gravity of the spacecraft must be known exactly. However, it would result in a more accurate determination on the non-gravitational forces.

If all other influences on the received signal are identified, the left over Doppler shift is can be used for the determination of the asteroid's absolute mass.

After the Rosetta flyby, the mass of the asteroid (21) Lutetia was estimated with (1.700 ± 0.017) x 10^{18} kg. The error of 1 % was mainly driven by three parameters. The Doppler shift was measured to (36.2 ± 0.2) mHz which corresponds to an error of 0.55 %. This error is descended from the error of the least-squares fit of the signal, which main cause is the frequency noise. The distance between spacecraft and asteroid during closest encounter was determined with an uncertainty of 0.24 %, which translates to (3168 ± 7.5) km in absolute values. Enhanced measurement methods for the range between spacecraft and asteroid could further diminish this uncertainty (see Chapter 5.2). The third main share of the uncertainty, with an error of 0.8 %, is the perturbation of the signal by Earth's atmosphere [12]. Further reduction of these uncertainties would then provide more accurate estimations for the mass of the asteroid.

The use of on-board radio science experiments is a reliable method for the mass estimation of asteroids with a very high accuracy. As for this purpose the standard communication system of the spacecraft can be used, it has only limited impact on the overall system design and requires no additional payload. Thus, it does not increase the weight of the spacecraft. Moreover, no additional development effort is necessary, as the hardware has been used many times. In combination with other scientific instruments of the spacecraft (e.g. Cameras, LiDAR), the RSE can be used for the determination of other asteroid properties, as will be presented in the following chapters.

5.2 Light Detection and Ranging

For an accurate determination of the position of an asteroid, both the distance between ground station and spacecraft (see Chapter 4) and the distance between spacecraft and asteroid must be known precisely. While the distance between spacecraft and Earth can be measured via ground based observations, on-board instrumentation is required for the range spacecraft – asteroid.

This can be done via *Light Detection and Ranging* methods, e.g. a laser altimeter. Thereby the spacecraft emits a laser pulse, which travels towards the target and is reflected on its surface. The reflected pulse is then again detected by a receiver of the spacecraft. The range R between spacecraft and asteroid can now be derived by multiplying the time difference Δt between emission and reception and the speed of light c. Finally this product must be divided by 2, as Δt accounts for the two-way travel time.

$$R = \frac{c\Delta t}{2} \tag{5-2}$$

Laser altimeters were on-board of several spacecrafts, like the asteroid sample return mission Hayabusa conducted by JAXA [9], or NASA's NEAR-Shoemaker mission [18]. The first European laser altimeter BELA will be on board the BepiColombo mission to Mercury.

Tab. 5-3: Parameter comparison of laser altimeter systems [19], [20]

Space Mission	Hayabusa	BepiColombo
Laser Altimeter	Hayabusa LIDAR	BELA
Wavelength [nm]	1064	1064
Range [km]	0.050 - 50	400 – 1055
Range Accuracy [m]	± 1	± 1.9
Pointing Uncertainty [µrad]	-	25
Beam Divergence (Full Cone) [µrad]	1700	50
Pulse Energy [mJ]	8	50
Repition Rate [Hz]	1	10
Power Consumption [W]	22	43.2
Weight [kg]	3.7	10.8

Table 5-2 presents relevant parameters of the Hayabusa and the BepiColombo LIDAR systems. Both of them use a Nd:YAG laser with a typical wave length of 1064 nm. Analyses have shown that especially this frequency provides a good signal-to-noise ratio and is therefore recommended for the application in laser altimeters [21]. This is especially important, due to the fact that the intensity of the received signal is generally much weaker than the intensity of the emitted pulse (see Fig. 5-3). As a result, the received pulse can be in the magnitude of the signal noise and a detection may not be possible anymore.

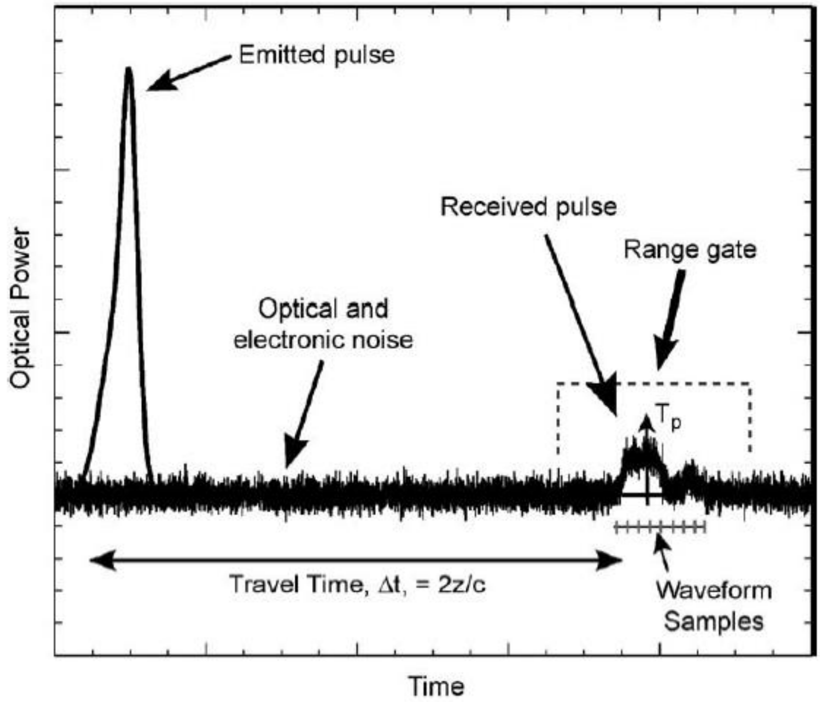

Fig. 5-3: Schematic of emission and time-delayed reception of a laser pulse [21]

The uncertainty in distance measurement is in the range of a few meters for both systems and would thereby – in conjunction with the data from the spacecraft tracking – allow a very precise estimation for the asteroid's position in the sky. However, the Hayabusa system is designed for measurements in a very close distance to the target with a maximum of about 50 km above the surface. This might be sufficient for a spacecraft orbiting an asteroid, but a flyby manoeuvre will normally demand a LIDAR system with a larger range. ESA's BELA system allows measurements in orbits of up to 1055 km. But as presented in Table 5-2, this requires a higher pulse energy and power consumption and consequently a larger payload. Considering Rosetta's flyby at asteroid 2867 Šteins, with a flyby distance of about 800 km [22], this system could be applied. Nevertheless, more powerful LIDAR systems are necessary for a wider range of flyby missions.

The applicable range of the LIDAR system is mainly governed by the energy of the incoming laser pulse [21]. If this value is too low, the spacecraft's receiver cannot detect the laser beam coming from the target's surface and a distance measurement is not possible. The energy of the backscattered pulse for a nadir-pointing can be calculated with the following equation [21]:

$$E_r = E_t T_r \frac{S}{z^2} \frac{A_N}{\pi} \tag{5-3}$$

The received pulse energy E_r depends on LIDAR system design parameters, in this case the emitted pulse energy E_t, the transmission of the receiver's optics T_r and the collecting area of the telescope S, as well as on the asteroid property of the albedo A_N of the reflecting surface.

Beyond that, the energy of the received signal decreases inversely with the square of the distance z.

The energy E of a single photon can be calculated by its frequency ν, respectively its wavelength λ and the Planck constant h [25]:

$$E = h\nu = h\frac{c}{\lambda} \tag{5-4}$$

The number of photons and consequently the received energy decreases with growing distance between spacecraft and target surface. For a detectable signal and thus a reliable measurement, the number of incoming particles should be in the range of $10^2 - 10^4$ photons per pulse [21].

In the following the performance and limits of the BepiColombo laser altimeter is evaluated in two cases:

- **Mercury Orbit:** BELA is installed on the BepiColombo spacecraft, which orbits Mercury with a 400 x 1500 km polar orbit [21].

- **(21) Lutetia Flyby:** A theoretical scenario, in which the BELA system is implemented into the Rosetta spacecraft. Hereby an application of this system during the (21) Lutetia flyby is evaluated and compared with the results of the Mercury orbit.

The data for the Mercury orbit corresponds to the exact scenario for this upcoming space mission. For the following considerations, the performance in a height of 900 km above the planet's surface is evaluated. The normal albedo A_N of Mercury is hereby estimated with a value of 0.26 [21].

The performance of the laser altimeter system is given by an energy contain of 50 mJ per emitted pulse, an achievable transmission of 63 % and a receiver with a telescope of 20 cm in diameter (see Tab. 5-3). These are the actual design parameters of the BepiColombo Laser Altimeter. Inserting the frequency of the used Nd:YAG laser and the *Planck Constant* into equation 5-4 we can derive an Energy E of 1.8670 x 10^{-16} mJ per single photon. Inserting the BELA system parameters and the values of the Mercury orbit in equation 5-3 result in an energy E_r of 1.0106 x 10^{-13} mJ per received laser pulse on the spacecraft. Dividing this value by the energy of a single photon results in about N = 541 detected photons per emitted pulse. For this calculation a parallel movement of both objects, with no relative velocity component in direction towards the target was assumed. Consequently, no frequency shifts between the emitted and received signal are present and thus, the energy of a single photons is equal for emission and reception. The number of detected photons lies in the above mentioned range and should thereby be detectable, which again allows reliable distance measurements.

The results of the Mercury orbit should now serve as a reference for further calculations.

The second case covers the possible application of the BELA during Rosetta's (21) Lutetia flyby. No laser altimeter system was on-board the Rosetta spacecraft, whereby this is only a theoretical consideration and should demonstrate the possible performance and limits of the BELA system in its current form.

Hereby the laser altimeter system parameters remain unchanged. However, the values for the distance between spacecraft and target (z = 3168 km) and the albedo of the surface (A_N = 0.208) are adjusted to the figures of the actual flyby in 2010 (see Fig. 5-3). Performing the same calculations like in the Mercury orbit case, we receive a detected energy of 6.5250 x 10^{-15} mJ, which corresponds to about 34 detected photons per pulse. These values are by far lower than in the first case, which is both due to the drastically increased distance between spacecraft and target and the slightly lower albedo of the surface. As a result, the laser pulse coming from (21) Lutetia's surface could probably not be clearly detected by the BELA system on the spacecraft.

In order to obtain accurate and reliable distance information under these circumstances, the performance of the current BELA system must be improved.

Taking into account equation 5-3, there are three main system parameters, which enable a higher received energy, namely the emitted pulse energy E_t, the transmission of the receiver's optics T_r and the collecting area of the telescope S. The remaining parameters of the equation are the albedo, which is an asteroid property and thereby cannot be modulated, and the flyby distance, which normally cannot be adapted arbitrarily, too.

A transmission coefficient of 63 % is at the upper limit of the realistically achievable [21] and probably allows no significant improvements in the near future. Consequently, the easiest way of adjusting the BELA system to possible asteroid flybys, is by increasing the emitted pulse energy E_r or the area S of the receiver telescope. Both ways have a significant impact on the spacecraft design, as they will result in a bigger LIDAR system with a higher mass. This again influences the design of the spacecraft and also the mission. An increase of the laser energy will additionally cause a higher power consumption of the laser altimeter.

Tab. 5-3 gives a short overview of necessary adjustments of these parameters for an application during the (21) Lutetia flyby. Hereby we approximately assume, that the detection of more than 100 photons per pulse is necessary for measurements [21]. Changing either the laser energy or the size of the telescope, would both demand values about three times higher than in the current system design. Especially the needed laser pulse energy of 150 mJ per pulse could be difficult to achieve.

However, the slight modification of both systems with a laser energy increase of about 30 % and the change in the telescope's diameter from 0.2 m to 0.3 m, would already allow LIDAR measurements at a distance of more than 3000 km.

Tab. 5-4: BELA Flyby Calculations [19]

BELA System Parameters	
Emitted Pulse Energy E_t [mJ]	50
Transmission Coefficient T_r [-]	0.63
Receiver Collecting Area S [m^2]	0.0314
Laser Wavelength λ [nm]	1064
Laser Frequency ν [Hz]	2.8176×10^{14} Hz
Planck Constant h [Js]	6.626×10^{-34}
Photon Energy E [mJ]	1.8670×10^{-16}
Mission Scenarios	
Mercury Orbit	
Distance Spacecraft – Target Surface z [km]	900 [21]
Surface Albedo A_N [-]	0.26 [21]
Received Pulse Energy E_r [mJ]	1.0106×10^{-13}
Number of Received Photons N [-]	541
(21) Lutetia Flyby	
Distance Spacecraft – Target Surface z [km]	3168 [12]
Surface Albedo A_N [-]	0.208 [26]
Received Pulse Energy E_r [mJ]	6.5250×10^{-15}
Number of Received Photons N [-]	34
(21) Lutetia Flyby with Improved LIDAR Capabilities	
E_t = 150 mJ	$N \approx 105$
S = 0.0962 m^2	$N \approx 107$
E_t = 65 mJ and S = 0.0707 m^2	$N \approx 102$

Apart from that, the width of the beam does not stay constant along its way. Although the divergence of a laser is naturally very small, the application for long distance measurements must consider this effect. Assuming a circular cross section of the emitted laser beam, its radius increases along the way and causes a footprint on the target's surface with a significantly bigger cross section than at the lens of the system. A larger footprint again causes a wider return pulse and consequently a lower intensity of the received laser beam. Thus, a very small divergence angle should be achieved. This requires high magnification and large optics [21], which again increases the instrument's mass.

The (full cone) divergence angle of the BELA system is kept very small at about 50 µrad. On Mercury, this causes a footprint of about 45 m in diameter for a signal emission 900 km above the surface. The footprint on (21) Lutetia would be about 158 m in diameter, due to the much larger distance. In case of planets or large asteroids like (21) Lutetia, with an average diameter of about 98.5 km [26], this widening would only constrain the spatial resolution and the mapping of the exact topography of the surface. An accurate distance measurement between the spacecraft and the footprint area on the surface should still be possible.

For smaller asteroids, in the range of a few hundreds of meters, it must be taken into account, that under the above mentioned parameters, e.g. a large distance between the two objects, the footprint size can reach the same magnitude as the asteroid dimensions. Thereby the spacecraft should perform the flyby in a closer distance, which would also improve the mass determination of the object (see Chapter 5.1).

In the same magnitude as the beam divergence is the pointing uncertainty of the BELA system (see Tab. 5-2). This uncertainty of 25 µrad could again lead to problems for the flyby at small objects and large distances. For bigger objects, this could again lead to problems if a high resolution mapping of the topography is desired, but should nevertheless provide accurate assumptions for the asteroid – spacecraft distance. As the applicable range of a LIDAR system is constrained, it may be only possible to use during the flyby around closest encounter, but not in the far field during approach or the postencounter phase. Consequently, the timespan for an efficient use of the LIDAR system is rather short, which therefore requires a precise orientation of the instrument during the flyby. Nevertheless, a laser altimeter can provide very accurate measurements and should be considered for such kind of missions.

5.3 Cameras

A crucial part in the process of orbit determination and propagation is an accurate knowledge of the position of an asteroid's centre of gravity. For this purpose, an orbiting spacecraft can conduct long-time RSE observations and measurements of the gravitational field, whereby conclusions about the centre of mass can be drawn. As the observational timeframe of a spacecraft flying past an asteroid is much shorter, the achievable resolution of the target's gravitational field is much lower [10]. This is sufficient for the determination of the asteroid's overall mass, but does not allow a very precise estimation for the position of the centre of gravity. In order to determine this property accurately, with measurements obtained during a flyby, Radio Science Experiments must be conducted in conjunction with a measurement of the size and shape (see Tab. 5-1). With these properties, the centre of figure can be computed and through measurements of the gravitational deflection of the spacecraft, the asteroid's centre of gravity can be estimated [10].

Through asteroid light curves, received by Earth-based observations, the shape and the rotational state of the target can be determined. From these measurements a 3-D shape model can be derived. However, these models are restricted to dimensionless, convex shapes with limited spatial resolution. Nevertheless, they provide qualitatively good assumptions. As they neither demand large observation facilities nor specialized instrumentation they will remiain the primary source for these properties [43].

Another possibility for the exploration of the spin state and the 3-D shape model is given by radar observations. Thereby a radio signal is sent to the target object and after a delay time its echo is detected. The distribution of the echo power and the Doppler frequency then allows estimations for the spin state and shape model. As the echo power scales inversely with distance to the fourth power, this method was mainly applied to Near-Earth Objects and lacks accuracy for targets in a larger distance [43].

A few ground-based telescopes and also the *Hubble Space Telescope* are able to resolve the apparent disk of the asteroids. This can be done via adaptive optics and a higher achievable angular resolution [43]. From several disk-resolved images and the knowledge of the rotation period, the spin-vector of the asteroid can be derived. As a result, the size and 3-D shape are obtained directly with this method and therefor provide a higher accuracy than the indirect reconstruction from light curve inversions [43].

Modern algorithms can use and combine data from several measurement techniques in order to estimate the size of an asteroid or even derive its 3-D shape. A high accuracy was shown by the *KOALA (Knitted Occultation, Adaptive-optics and Lightcurve Analysis)*, which estimated the size and shape of (21) Lutetia with input parameters collected before the Rosetta visit and afterwards compared it with measurements obtained during the flyby. The *KOALA* algorithm makes use of the spin and 3-D shape estimations given by light curve observations and combines this data with direct measurements of the apparent size and shape of the object, provided by observations during stellar occultation and disk-resolved images [43]. The primary result of this method are estimations for the spin-state, the spin-vector and the 3-D shape of the asteroid.

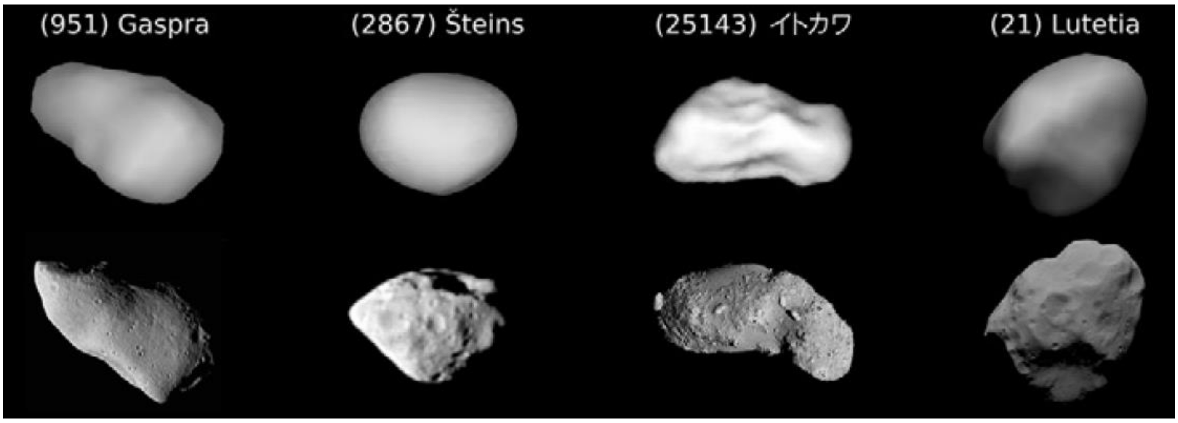

Fig. 5-4: Shape models derived from Earth-based observations (top) and S/C (bottom) [43]

As depicted in Fig. 5-4, more precise estimations for the size and shape can be derived from a spacecraft visiting the asteroid. During its (21) Lutetia flyby, Rosetta took 462 images with its *OSIRIS (Optical, Spectroscopic and Infrared Remote Imaging System)* system, from about 9 hours before to 16 minutes after closest approach [41]. The flyby geometry allowed an observation of the asteroid's northern hemisphere, while the southern part could not be imaged. Nevertheless, the pictures cover more than 50 % of the body's surface and allow a resolution between 5000 to 60 meter per pixel, if (21) Lutetia fills the camera's field of view [42].

The enhanced shape model with image data from the flyby was created by the combination of two techniques. For the observable northern hemisphere, 60 images, taken during the nine-hour observation period of the flyby, were evaluated. Using methods of *Stereophotoclinometry* and *Stereophotogrammetry* (see [44]) a detailed 3-D shape model could be created for this region of the asteroid. The shape model of the southern hemisphere, which was only partially visible from Rosetta, combines the inversion of 50 photometric light curves and contours of adaptive optics images, both detected from ground-based observatories [42]. These measurements from Earth were applied to the *KOALA* algorithm and computed into a 3-D shape model of the southern hemisphere. The volume error for this part of the body depends mainly on the existence and accuracy of ground-based adaptive optics images from viewing directions which are not observable from the spacecraft and the pre flyby adaptive optics and light curves approach model (*KOALA)* [42].

For the northern part of the asteroid two different shape models exist. The first one is computed with the *KOALA*-code and thereby solely uses Earth-based measurements, while the second one is derived from Rosetta's images only. A comparison shows that both shape assumptions have a very good agreement with an overall deviation of only 5 % within this area [42]. As the southern hemisphere of the (21) Lutetia could not be imaged during the flyby, its shape model is solely based on *KOALA*-calculations. But as both models show a very good agreement, we can assume that the prediction for the shape of the southern part is quite accurate.

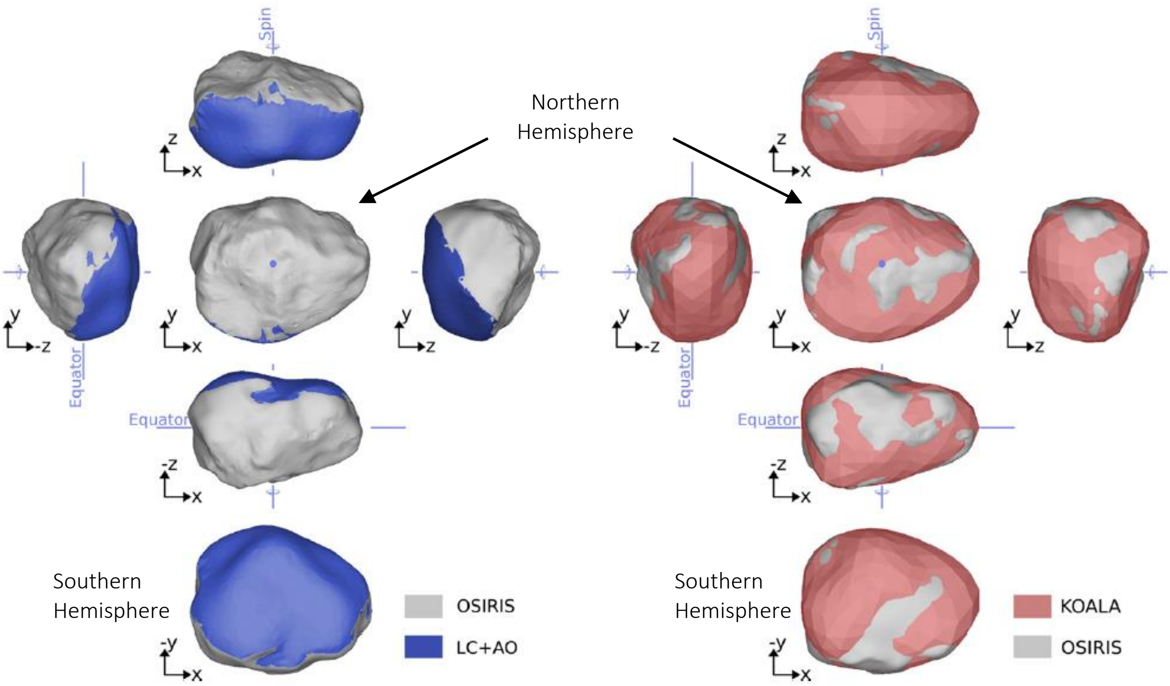

Fig. 5-5: Comparison of (21) Lutetia 3-D models [43]

Fig. 5-5 presents a schematic comparison between the shape assumptions from ground and the one gathered during flyby. The left plot shows the contour data based on the flyby (grey) and the data from ground-based observations (blue), in this case the evaluation of light curves and images. The right plot shows the difference between the pre flyby *KOALA*-model (red) and the post flyby model (grey) which incorporates the images taken by Rosetta. The red colour indicates areas, where the radii of the *KOALA*-model are larger than those of the *OSIRIS*-model.

A comparison between the absolute dimensions and the spin axes is given in Tab. 5-4. Thereby *OSIRIS* represents the data of the model which incorporates the flyby measurements whereas *KOALA* uses only the Earth-based measurements, which were available before Rosetta mission. The *KOALA*-results show a principally good agreement with the *OSIRIS*-data, although the uncertainties could be decreased. This accounts especially for the diameters a and b, while the diameter c could also not be determined very precisely. The reason for the c-inaccuracy of the *KOALA*-simulations lies within the input data. Although this data was collected over multiple epochs, the perspective from Earth allowed mainly views from high southerly or high northerly sub-Earth latitudes [43]. Consequently, this value cannot be constrained sufficiently from Earth-based observations. This uncertainty can also not be reduced through the images of Rosetta, as this side of the asteroid was almost not visible.

For future flyby missions, which intend to estimate the shape and dimensions of the asteroid, a combination of both methods seems promising. As the *KOALA*-algorithm provides a very accurate shape model, based on observations from Earth, it can serve as preliminary assumption.

However, some parts of the asteroids will not be visible with these methods and will cause inaccuracies, like the c diameter of (21) Lutetia. A spacecraft on a flyby mission could then follow a trajectory around the target, from where these parts can be explored, which would help to complete the shape model. Based on this shape model and in combination with the RSE-data, the asteroid's centre of gravity can be determined.

Tab. 5-5: Dimension estimations for (21) Lutetia [42], [43]

Technique	OSIRIS	KOALA
Diameter a [km]	121 ± 1	124 ± 5
Diameter b [km]	101 ± 1	101 ± 4
Diameter c [km]	75 ± 13	93 ± 13
Mean Diameter d [km]	98 ± 2	105
Volume V [km^3] x 10^5	5.0 ± 0.4	
Spin Vector Longitude λ [°]	52.2	52
Spin Vector Latitude β [°]	-7.8	-6

5.4 Thermal-Infrared Spectrometer

For some asteroids, non-gravitational forces can have a significant impact on their trajectory. The *Yarkovsky* effect can thereby serve as an example, as this one is often the predominant non-gravitational force acting upon an asteroid's orbit [10]. The varying insolation on the day- and night-side of the object causes temperature differences on its surface. Consequently, the irregular emission of absorbed solar radiation leads to a small force which still can result in a significant change of the semi major axis. This deflection is especially relevant for asteroids with a diameter of less than 20 km [10] and can lead to drifts of the semi major axis in the range of $10^2 - 10^3$ m/year [9].

In order to estimate the magnitude and direction of this force, an accurate temperature map and the knowledge of the thermal inertia of the asteroid's surface is required. In conjunction with the rotational period of the target, an approximation of the outcome of the *Yarkovsky* effect is then possible.

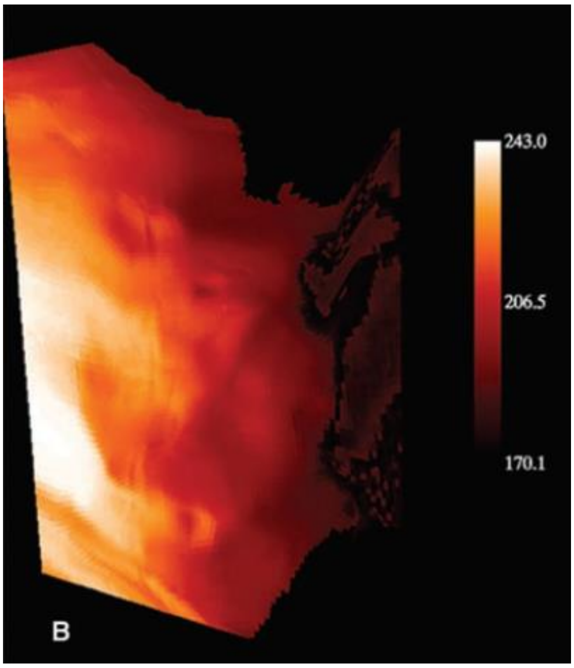

Fig. 5-6: Surface temperature of (21) Lutetia, mapped by Rosetta [45]

Equipping a spacecraft with a thermal-infrared spectrometer would allow to determine the thermal inertia and temperature distribution. For *Near-Earth Objects*, thermal emission is starting to become significant at around 2-3 µm, depending on properties like the albedo or the heliocentric distance [9]. The instrument should be capable to measure temperatures in the range between 100 and 400 K, in order to account for the surface of both the day- and night-side [10]. Mid-infrared observations would allow a determination of the thermal inertia. This property can be used to estimate the time it takes for the surface to heat up or cool down, and is therefore also useful to estimate the thermal emission. Thereby, the heating and cooling of the surface, due to solar radiation and the rotation of the asteroid, can be estimated and the orbited change can be predicted.

The Rosetta spacecraft was equipped with the *VIRTIS- (Visible, InfraRed and Thermal Imaging Spectrometer)* instrument. This system consists of two independent channels. *VIRTIS-M* can obtain hyperspectral images in the range from 0.25 to 5.1 µm. The *VIRTIS-H* has a high resolution infrared spectrometer and thereby allows the temperature mapping of the surface. It is calibrated for a range between 2 to 5 µm with a spectral resolution of about 3000 and can detect temperature differences smaller than 1 K, which allows an accurate modelling of the temperature distribution and the thermal inertia [10], [45].

This technique, applied during the (21) Lutetia flyby, revealed a temperature span of 170 to 245 K for the explored area of the surface [45]. However, due to the orientation of (21) Lutetia and the flyby geometry only about 50 % of the asteroid could be imaged.

For a precise investigation on the *Yarkovski* effect, the spatial resolution of the temperature mapping should be in the range of a few meters. The *VIRTIS* system of Rosetta is able to achieve a spatial resolution of 250 µrad [45], which corresponds to a footprint of about 13.8 m in diameter if applied to the closest encounter at (21) Lutetia. For a detailed evaluation of the *Yarkovski* effect in future missions, a higher spatial resolution should be attempted.

5.5 Deployable Probes

The most accurate measurements of asteroids can be made through an orbiting spacecraft. Beyond that, placing a separate lander on the object's surface can even enhance the collected data and allow further experiments. However, this is a very complex mission scenario, as the lander, which is normally equipped with a very sensitive payload, must touch down, both at the right spot, which allows the planned experiments, and with the right speed, which does not harm the instruments. On the one hand, this increases the complexity and costs of such a mission, but on the other hand also allows long-time studies of the target, which are not possible with a flyby. The following chapter now presents two approaches for flyby manoeuvres which make use of a deployable payload. Thereby the resulting timespan of the asteroid observation can be increased without significantly higher complexity or costs.

5.5.1 Swarm Flyby Gravimetry

The accurate determination of an asteroid's gravitational field normally requires sophisticated measurements, performed by an orbiting spacecraft. As the spacecraft circles around the object, data from various positions all around the target can be collected, which allows a detailed

3-D resolution of the body's gravity. However, a spacecraft flying past can only measure this property with a much lower accuracy.

A method, which does not require dedicated landing modules, but is still able to explore the asteroid's gravity field and mass distribution, is the *Swarm Flyby* approach. Thereby the host spacecraft releases a number of small probes (see Fig. 5-7) during, or shortly prior to the flyby. These probes can be built very simple as they only need a transponder, so their position can be tracked from the host spacecraft.

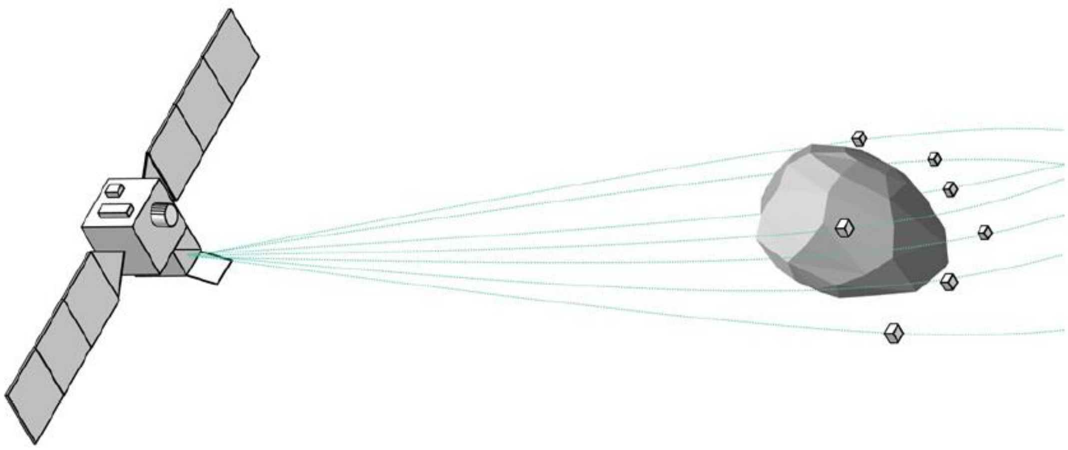

Fig. 5-7: Ejection of several probes from the host spacecraft during the flyby [40]

The probes can approach the target from different ranges and directions, controlled by their injection from the host spacecraft. The individual probes pass the asteroid on a distinctive trajectory, whereby each of them performs an independent flyby. The gravitational field of the centre body again acts upon the small masses of the probes and deflects their path. The host spacecraft can track the movement of the ejected probes, especially their relative position before and after the closest encounter with the asteroid, and can send this data to Earth. The trajectories of each probe can now be evaluated and computer software can be applied to find the best-fit solution for the asteroid's gravity field [40].

The accuracy of this method is governed by the uncertainty of the probe tracking from the host spacecraft. Moreover, a higher number of probes and variety of approaching angles increases the preciseness of the results. Theoretically 1 to 3 ideally ejected and placed probes can already provide very good estimates. However, in order to account for deployment errors and deviations from the ideal trajectory, about 10 to 12 probes should be considered [40].

Applying this method, the number and quality of measurements can be increased quite easily, allowing the exploration of the asteroid's gravitational field with several probes from different angles. This could significantly augment the gravimetry measurements of a classical flyby, without the need for an additional lander or endangering the mission via a low altitude pass of the host spacecraft. Beyond that, the probes do not need to be extremely sophisticated, as they only must be trackable. This reduces the on-board instruments to a Radio-Science Transponder. Thereby they can be rather cheap, small and easily accommodated on-board a spacecraft.

Analysis show that through applying this method, the point mass term of the target can be estimated with an accuracy of up to 5 % [40]. Although this method has never been applied for the exploration of asteroids, its possibilities and performance should be further examined, as it offers the chance to increase amount of data quite easily.

5.5.2 Asteroid Marker

So far, all illustrated methods determine asteroid properties, in particular the position, for only one or a few points in time. This may cause inaccuracies within the long-term propagation of asteroid orbits, which is based on this constrained data.

However, a continuous tracking would provide the up to date position, whereby the orbit propagation could be adapted and inaccuracies reduced. A similar scenario is envisaged for the encounter of Apophis in 2029 [48].

Through a flyby mission, the spacecraft could again deploy a probe towards the target. Contrary to the *Swarm Flyby Gravimetry*, the probe must now reach the surface of the asteroid and remain there permanently. Through the landing of a laser, radar or radio reflector or transponder on the surface, the asteroids position could be observed almost continuously over a long time span. Here, radar techniques seem better suitable, than optical measurements [48] and would allow position determinations with an accuracy comparable to the spacecraft tracking accuracy based on *Radio Science Experiments* (see Chapter 4).

6 Conclusion and Outlook

In this thesis a number of on-board instruments, which could be implemented into a flyby mission were evaluated. Thereby the main aspect was their possible contribution to an improvement in position and consequently orbit knowledge of an asteroid. This chapter will now summarize the main results of the thesis and give a suggestion for a reasonable spacecraft payload.

While the commonly used radiometric range and Doppler measurements provide precise estimations for the velocity and distance in the line-of-sight, with uncertainties of only a few meters they show inaccuracies in the angular position determination of the spacecraft. During the flyby phase, a tracking of the spacecraft with delta-DOR methods should be considered, as it would provide a very high angular resolution, which causes inaccuracies of only a few hundred meters, even in very large distances. The application of Delta-DOR techniques is more complex than the traditional radiometric techniques, but has been applied many times and shows accurate and reliable results.

The mass of the asteroid is of high interest for the orbit propagation and should be definitely determined as accurate as possible. Previously performed flybys, like at (21) Lutetia, show that a very precise determination of this parameter is still possible, given the limited amount of observation time during a flyby. The method of choice for these investigations are *Radio Science Experiments (RSE).* In its simplest form, no additional payload or instruments are necessary, as the communication system of the spacecraft can be used for these experiments. The crucial parameter for an accurate and reliable is the frequency shift of the signal. The use of dual-band link with high frequencies (X- and Ka-band) is highly recommended, as they can both provide a higher accuracy and are less effected by perturbations of the atmosphere. If the mission design allows it, a close encounter with the spacecraft moving along the line-of-sight from Earth, should be preferred. The *Radio Science Experiments* can be augmented by an additional accelerometer. Non-gravitational perturbations, mainly the solar radiation pressure, can thus be distinguished from the asteroids attraction, which again allows higher accuracies. This can be an option for flybys, where a significant influence of solar radiation pressure can be expected, e.g. at small asteroids with low masses or flybys in large distances. The respective technique is largely available and also small accelerometers with a low mass show accurate results.

For range measurements between the spacecraft and the asteroid, laser altimeter systems promise high-quality results. The distance can be determined with a few meters in precision. Although, already developed LIDAR systems like BELA can provide a possible heritage. Their performance, mainly the energy of the laser beam, will have to be increased for most asteroid flyby missions. Special emphasis must be put on a precise pointing and orientation of the system, especially in large distances from the asteroid. This is due to the fact, that a flyby allows only a very limited time span for observations and therefore only few single measurements can be conducted. Consequently, the beam divergence and the pointing uncertainty of current LIDAR system will need an improvement for future asteroid flyby missions.

Additionally, the spacecraft should be equipped with several optical cameras. They can serve for navigation purposes, which is especially relevant for the approach of the asteroid. Beyond that high resolution cameras can provide a 3-D shape of the asteroid with high accuracy. As a flyby cannot observe the whole surface of the asteroid, the use of cameras, in conjunction with 3-D shape modelling techniques, based on ground based observations (*KOALA)* is an option. These computations provide quite accurate shape and size assumptions, although they are based on pre-flyby data. As seen in Chapter 5.3, the flyby could be used to determine the dimension of the asteroid in directions, which cannot, or can only rarely be seen from ground, and thereby lack of accuracy. The trajectory of the flyby would consequently need to consider this.

As the orbit of asteroids, especially of rather small ones (diameter < 20 km) can be highly affected by non-gravitational forces, mainly the *Yarkovsy* effect, an estimation for this parameter would help to propagate the orbit sufficiently. On-board thermal-infrared spectrometers can provide estimates for the thermal inertia and the temperature map and could thereby help to assess the influence of the non-gravitational forces.

All the mentioned techniques and instruments have already been applied and their reliability was proven. Further modifications or increases in performance will probably be necessary for some asteroid flyby missions, but a broad heritage is available and can be used in future.

Although the methods of *Swarm Flyby Gravimetry* and an *Asteroid Marker* have not been applied yet, they promise significant enhancements and deserve further investigation. Especially the latter one would provide long term observation data and precise estimations for the position and the orbit of the asteroid.

Most of the techniques and instruments, which are necessary for the accurate determination of an asteroid's position are already available. With further improvements and mission specific modifications, asteroid ephemerides determinations with uncertainties of only a few hundred meters should be possible.

The following list now gives a final overview of the spacecraft instrumentation and mission design, which is highly recommended for an asteroid flyby mission with the purpose of an orbit knowledge improvement:

- **Delta Differential One-Way Tracking:** This enhanced spacecraft tracking method should be considered for future asteroid missions, as the position of the spacecraft can be measured with an accuracy of a few meters in range and a few hundreds of meters in the angular (plane of sky) position. The latter can provide an up to 120000 times higher accuracy than Range Rate measurements, or a 1200 times higher accuracy compared to on-board, optical methods. This would allow a complete and precise determination of the spacecraft's position with an uncertainty of only a few hundreds of meters.

- **Radio Science Experiments:** A mass determination of the asteroid via Radio Science Experiments is highly recommended, too. The uncertainty of the asteroids mass can be limited to nearly 1 %, which is a 10 to 15 times higher accuracy than the one achievable from Earth-based observations only.

- **Light Detection and Ranging:** A high performance LiDAR-system on-board the spacecraft allows spacecraft-asteroid distance measurements with an error in the range of a few meters. This error is normally much smaller than the uncertainty in the spacecraft tracking data. Combined with this tracking data, obtained through delta-DOR methods, the position of the asteroid can now be determined with an accuracy of a few hundreds of meters

- **Optical Cameras:** The spacecraft should be equipped with at least one camera. This can be used for navigation purposes, especially in critical flight phases like the asteroid approach or flyby. Beyond that, the shape and dimensions of the asteroid can be measured with an uncertainty of only a few percent.

A Appendix

A.1 References

[1] Thornton C. L., Border J. S.: *Radiometric Tracking Techniques for Deep Space Navigation*, John Wiley & Sons. Inc., New Jersey, 2003

[2] Турышев В. Г.: *Basics of Spacecraft Navigation Lecture 9.0 – Principles, Methods and Observables*, California Institute of Technology, Pasadena, 2003

[3] Maddè R., Morley T., Abelló R., Lanucara M., Mercolino M., Sessler G., de Vicente J.: *Delta-DOR – A New Technique for ESA's Deep Space Navigation*, ESA Bulletin 128 – Directorate of Operations & Infrastructure, Darmstadt, 2006

[4] James N., Abelló R., Lanucara M., Mercolino M., Maddè R.: *Implementation of an ESA Delta-DOR Capability*, Acta Astronautica 64, 2009

[5] Iess L., Di Benedetto M., Marabucci M., Racioppa P.: *Improved Doppler Tracking Systems for Deep Space Navigation*, Dipartimento di Ingegneria Meccanica e Aerospaziale, Sapienza, Università di Roma, Rome, 2014

[6] Barbaglio F.: *Precise Angle and Range Measurements: Advanced Systems for Deep Space Missions*, PhD Thesis, Università di Roma, Rome, 2012

[7] Iess L., Di Benedetto M., Marabucci M., Racioppa P.: *ASTRA – Interdisciplinary Study on Enhancement of End-to-End Accuracy for Spacecraft Tracking Techniques*, Acta Astronautica 94, 2012

[8] Butkovic M., *ESTRACK: Technical Aspects, Performance, Limitations and Future Prospects*, Seminar for "Autonomous Spacecraft Navigation – New Concepts, Technologies & Applications for 21st Century", Bad Honnef, 2015

[9] Perna D., Barucci M. A., Fulchignoni M., Fornasier S.: *NEOShield – A Global Approach to Near-Earth Object Impact Threat Mitigation – D2.3: Instrumentation Designs for A Mitigation Precursor and Demo Mission*, DLR, 2012

[10] Bancelin D., Birlan M., Fornasier S., Fulchignoni M., Hestroffer D., Thuillot W.: *NEOShield – A Global Approach to Near-Earth Object Impact Threat Mitigation – D2.2 Report on Requirements for Mitigation Precursor Reconnaissance*, DLR, 2012

[11] Andert T. P.: *Masses of Small Bodies – Mass Estimation of Small Solar System Bodies using Radio Science Data from Close Flybys*, PhD Thesis, Universität zu Köln, 2010

[12] Pätzold M., Andert T. P., Asmar S. W., Anderson J. D., Barriot J. P., Bird M. K., Häusler B., Hahn M., Tellmann S., Sierks H., Lamy P., Weiss B. P.: *Asteroid 21 Lutetia: Low Mass, High Density*, Science Vol. 334, 2011

[13] Hilton J. L.: *Asteroid Masses and Densities*, U.S. Naval Observatory, 2002

[14] Pätzold M., Andert T. P., Häusler B., Tellmann S., Anderson J. D., Asmar S. W., Barriot J. P., Bird M. K.: *Pre-Flyby estimates of the Precision of the Mass Determination of Asteroid (21) Lutetia from Rosetta Radio Tracking*, Astronomy and Astrophysics Vol. 518, 2010

[15] Koschny D.: *Near-Earth Objects for Engineers and Physicists (Version 1.2)*, Lecture Notes, Technische Universität München, 2015

[16] Pätzold M., Andert T. P., Asmar S. W., Anderson J. D., Barriot J. P., Bird M. K., Häusler B., Hahn M., Tellmann S., Sierks H., Lamy P., Weiss B.P.: *Asteroid 21 Lutetia: Low Mass, High Density – Online Supporting Material*, Science Vol. 334, 2011

[17] Bruzzi J. R., Strohbehn K., Boone B. G., Kerem S., Layman R. S., Noble M. W.: *A Compact Laser Altimeter for Spacecraft Landing Applications*, The John Hopkins APL Technical Digest Volume 30, 2012

[18] Cheng A. F., Barnouin-Jha O., Zuber M. T., Veverka J., Smith D. E., Neumann G. A., Robinson M., Thomas P., Garvin J. B., Murchie S., Chapman C., Prockter L.: *Laser Altimetry of Small-Scale Features on 433 Eros from NEAR-Shoemaker*, Science Vol. 292, 2001

[19] Michaelis H., Spohn T., Thomas N., Seiferlin K., Oberst J., Behnke T., Hilchenbach M., Roll R., Schreiber U.: *The BELA – The First European Planetary Laser Altimeter*, Presentation 15th Laser Ranging Workshop, Canberra, 2006

[20] Mizuno T., Tsuno K., Okumura E., Nakayama M.: *LIDAR in Hayabusa Mission*, Presentation Institute of Space and Astronautical Science JAXA

[21] Thomas N., Spohn T., Barriot J. P., Benz W., Beutler G., et al.: *The BepiColombo Laser Altimeter (BELA): Concept and Baseline Design*, Planetary and Space Science 55, 2007

[22] Morley T., Fertig J.: *2867 Šteins Orbit Determination*, Issue 2.1, ESA – Directorate of Operations and Infrastructure, 2009

[23] Gardner C. S.: *Ranging Performance of Satellite Laser Altimeters*, University of Illinois, Department of Electrical and Computer Engineering, 1992

[24] Zuber M. T., Smith D. E., Solomon S. C., Muhleman D. O., Head J. W., et al.: *The Mars Observer Laser Altimeter Investigation*, Journal of Geophysical Research Vol. 97, 1992

[25] Skinner R.: *Relativity for Scientists and Engineers*, Dover Pubn Inc., Mineola, 2014

[26] Mueller M., Harris A. W., Bus S. J., Hora J. L., Kassis M., Adams J. D.: *The Size and Albedo of Rosetta Flyby Target 21 Lutetia from new IRTF Measurements and Thermal Modeling*, Astronomy & Astrophysics, 2005

[27] Carr M. H.: *Asteroids, Comets and Planet Formation*, JPL the Geology of Terrestrial Planets, Washington DC, 1984

[28] NASA – JPL: *http://neo.jpl.nasa.gov/stats/,* March 23rd, 2016, 5:11 pm

[29] ESA*: http://www.esa.int/spaceinimages/Images/2010/05/Asteroid_Flury*, March 25th, 2016, 10:44 am

[30] TOTAS: *http://vmo.estec.esa.int/totas/mover.php?id=548,* March 25th, 2016, 11:13 am
[31] NASA – JPL: *http://neo.jpl.nasa.gov/stats/,* March 25th, 2016, 1:14 pm
[32] NASA – JPL: *http://nssdc.gsfc.nasa.gov/planetary/factsheet/asteroidfact.html*, March 25th, 2016, 5:31 pm
[33] ESA – Rosetta Mission: *http://sci.esa.int/rosetta/43356-2867-steins,* March 25th, 2016, 6:06 pm
[34] NASA – JPL: *http://stardust.jpl.nasa.gov/news/news94.html,* March 25th, 2016, 6:19 pm
[35] Curtis H.: *Orbital Mechanics for Engineering Students*, Elsevier Butterworth-Heinemann, Oxford, 2005
[36] Desmars J., Bancelin D., Hestroffer D., Thuillot W.: *Asteroid Ephemerides Final Report*, IMCCE – Paris Observatory, 2010 (Update: January 2011)
[37] NASA: *http://nssdc.gsfc.nasa.gov/planetary/factsheet/sunfact.html,* March 26th, 2016, 1:42 pm
[38] NASA: *http://nssdc.gsfc.nasa.gov/planetary/factsheet/jupiterfact.html,* March 26th, 2016, 1:51 pm
[39] ESA: *http://sci.esa.int/rosetta/47448-rosetta-status-report-no-141/,* March 26th, 2016, 2:14 pm
[40] Atchison J., Mitch R., Rivkin A.: *Swarm Flyby Gravimetry*, NIAC Phase I Final Report, Applied Physics Laboratory, John Hopkins University, 2015
[41] Schulz R., Sierks H., Küppers M., Accomazzo A.: *Rosetta Flyby at Asteroid (21) Lutetia: An Overview,* Planetary and Space Science, 2011
[42] Sierks H., Lamy P., Barbieri, Koschny D., et al.: *Images of Asteroid 21 Lutetia: A Remnant Planetesimal from the Early Solar System*, Science Vol. 334, 2011
[43] Carry B., Kaasalainen M., Merline W. J., Müller T.G., et al.: *Shape modeling technique KOALA validated by ESA Rosetta at (21) Lutetia*, Planetary and Space Science 66, 2012
[44] Gaskell R. W.: *Mapping Small Bodies with Stereophotoclinometry*, Planetary Science Institute, Tucson,
[45] Zou X., Li C., Liu J., Wang W., Li H., Ping J.: *The Preliminary Analysis of the 4179 Toutatis Snapshots of the Chang'E-2 Flyby,* Icarus Vol. 229, 2014
[46] Discovery News: *http://news.discovery.com/space/astronomy/chinese-moon-probe-buzzes-asteroid-121214.htm,* March 27th, 2016, 6:27 pm
[47] Gennery D. B.: *Scenarios for Dealing with Apophis*, Planetary Defense Conferencce, Washington DC, 2007
[48] Hinglais E.: *Apophis 2029 Mission, A CNES Engineering Study – ApEx Mission (Apophis Explorer),* Presentation, Flagstaff, 2013
[49] Prado J. Y. Hinglais E., Lopes L., Martin T., et al.: *Apophis Explorer, Taking the Opportunity of its 2029 Flyby for a Characterization Mission,* Centre National d'Etude Spatiales, Tolouse, 2015
[50] Prado J. Y.: *Apophis 2029 – A Unique Mission Opportunity*, CNES – Presentation, Tolouse, 2010

[51] ZME Science: *http://cdn.zmescience.com/wp-content/uploads/2014/11/21JanRosettaSpaceWEB.jpg,* March 28th, 2016, 8:49 pm

[52] NASA: *http://science.nasa.gov/science-news/science-at-nasa/2008/30jun_tunguska/,* March 29th, 2016, 10:39 am

[53] Discovery News: *http://news.discovery.com/space/asteroids-meteors-meteorites/russian-meteor-chelyabinsk-asteroid-had-violent-past-140522.htm,* March 29th, 2016, 10:43 am

[54] SMPAG: *http://www.cosmos.esa.int/web/smpag,* March 29th, 2016, 11:17 am

[55] Bashkaran S.: *Autonomous Navigation for Deep Space Missions,* SpaceOps Conference, Stockholm, 2012

[56] Morley T., Budnik F., Croon M., Godard B.: *Rosetta Navigation for the Flyby of Asteroid (21) Lutetia,* International Symposium on Space Flight Dynamics, Pasadena, 2012

[57] Scheeres D. J., Ostro S. J., Hudson R. S., DeJong E. M., Suzuki S., *Dynamics of Orbits Close to Asteroid 4179 Toutatis*, Icarus Vol. 132, 1998

[58] ESA: *http://www.esa.int/Our_Activities/Space_Science/Rosetta/Encounter_of_a_different_kkin_Rosetta_observes_asteroid_at_close_quarters,* March 29th, 2016, 5:58 pm

[59] Solarviews: *http://solarviews.com/eng/annefrank.htm,* March 29th, 2016, 6:45 pm